

Analysis and optimization with the Kullback-Leibler divergence for misfire detection using estimated torque*

Daniel Eriksson, Lars Eriksson, Erik Frisk, and Mattias Krysander

*Division of Vehicular Systems, Department of Electrical Engineering
Linköping University SE-581 33 Linköping, Sweden
E-mail: {daniel.eriksson, lars.eriksson, erik.frisk, mattias.krysander}@liu.se
Technical report: LiTH-ISY-R-3057*

March 6, 2013

Abstract

Engine misfire detection is an important part of the On-Board Diagnostics (OBDII) legislations to reduce exhaust emissions and avoid damage to the catalytic converters. The flywheel angular velocity signal is analyzed, investigating how to use the signal in order to best detect misfires. An algorithm for engine misfire detection is proposed based on the flywheel angular velocity signal. The flywheel signal is used to estimate the torque at the flywheel and a test quantity is designed by weighting and thresholding the samples of estimated torque related to one combustion. During the development process, the Kullback-Leibler divergence is used to analyze the ability to detect a misfire given a test quantity and how the misfire detectability performance varies depending on, e.g., load and speed. The Kullback-Leibler divergence is also used for parameter optimization to maximize the difference between misfire data and fault-free data. Evaluation shows that the proposed misfire detection algorithm is able to have a low probability of false alarms while having a low probability of missed detections.

*This work has been supported by Volvo Cars.

Contents

1	Introduction	3
2	Vehicle control system signals	3
3	Analysis of the flywheel angular velocity signal	5
4	The Kullback-Leibler divergence	10
5	Torque estimation based on the angular velocity signal	11
5.1	Analyzing misfire detectability performance of estimated torque signal	14
5.1.1	Signal distribution at one operating point	14
5.1.2	Analyzing signal distribution using the Kullback-Leibler divergence	19
6	An algorithm for misfire detection	23
6.1	Algorithm outline	23
6.2	Design of test quantity	23
6.3	Thresholding	27
7	Evaluation of the misfire detection algorithm	29
8	Conclusions	36
9	Future works	36

1 Introduction

Engine misfire detection is an important part of the On-Board Diagnostics (OBDII) legislations to reduce exhaust emissions and avoid damage to the catalytic converters, see [13]. Misfire refers to an incomplete combustion inside a cylinder and can be caused by many different factors, for example, a failure in the ignition system or a clogged fuel injector, see [8]. The On-Board Diagnostics system is required to both detect misfires and identify in which cylinder the misfire occurred, see [8] and [17].

An overview of engine misfire detection research is found in [13]. There are several approaches to detect misfires using different types of sensors, e.g., ion current sensors, see [12], or crankshaft angular velocity measured at the flywheel, see [15], [14], and [16]. Misfire detection based on torque estimation using the flywheel angular velocity signal has been studied in, e.g, [4], [10], and [17]. Detecting misfires is a non-trivial problem which is complicated by, for example, changes in load, speed, and flywheel manufacturing errors, see [14] and [10].

As a tool during the design process of the misfire detection algorithm, the Kullback-Leibler divergence is proposed to evaluate misfire detectability performance [5]. The Kullback-Leibler divergence can be used to quantify the separation of two distributions, for example, to evaluate the misfire detectability performance before a test quantity is designed or when optimizing algorithm parameters to maximize the separation. Other examples where the Kullback-Leibler divergence is used for quantifying diagnosability performance are [6] and [7].

A misfire detection algorithm is proposed based on torque estimation at the flywheel using flywheel angular velocity measurements. The test quantity is designed by weighting the estimated torque related to one combustion such that the distributions of fault-free data and misfire data are as separated as possible. To handle variations of the estimated torque due to cold starts and varying load and speed, the parameters of the misfire detection algorithm depend on the operating point. Parameterization of the misfire detection algorithm is performed automatically given training data and evaluations show that misfires are detected with low probability of missed detections while having few false alarms.

A short presentation of the vehicle control system signals is given in Section 2 and an analysis of the flywheel angular velocity signal and the effects of misfire is presented in Section 3. In Section 4, the Kullback-Leibler divergence is described which is used to analyze misfire detectability performance. The flywheel angular velocity signal is used to estimate the torque at the flywheel in Section 5 and the estimated torque is analyzed using the Kullback-Leibler divergence. Then, the misfire detection algorithm is presented in Section 6 and evaluated in Section 7. Finally, the conclusions are presented in Section 8 and future works in Section 9.

2 Vehicle control system signals

A list of the vehicle control system signals and variables used by the misfire detection algorithm is presented in Table 1. All data used in this work are measured from real cars from Volvo. The flywheel angular velocity signal is used to detect misfires and the crank counter, load, speed, and the catalytic converter warming flag are used to identify the operating point of the engine, in which cylinder the combustion occurs, and if it is during a cold start or not. All signals are sampled crankshaft angle synchronous, instead of time synchronous, at the same rate which depends on the number of cylinders.

During the data collection, misfires have been injected by interrupting the combustion in different cylinders. The misfires are occurring with fixed intervals between cycles while switching which cylinder that is misfiring. Note that it is not known if the data contains more misfires than the injected misfire. Therefore, all samples not related to an injected misfire is assumed

fault-free. Thus, only intermittent misfires are analyzed in this work and no occurrence of a constant misfiring cylinder. However, intermittent misfires are considered more difficult to detect since the fault appears and disappears randomly.

Table 1: A list of vehicle control system signals used by the misfire detection algorithm.

Signal	Unit
Flywheel angular velocity signal	$\mu s/\Delta\theta$
Crank counter	-
Speed	rpm
Load	g/rev
Catalytic converter warming flag	-

The flywheel angular velocity signal is the measured time period for different angular intervals of the flywheel, see [9]. The angular intervals are determined and limited by the angles between the teeth on the flywheel, which are usually 6° . Two teeth are removed to keep track of the angle of the flywheel as shown in Figure 1. The available flywheel angular velocity signals have the lower resolution of 30° for five cylinder engines and 36° for six cylinder engines, see Table 2. This results in 20 samples per cycle for five cylinder engines and 24 samples per cycle for six cylinder engines. In both cases, this results in four samples per cylinder combustion.

Table 2: A summary of the flywheel angular velocity signal resolution for different number of cylinders.

Num. cylinders	Resolution	samples/revolution	samples/cycle	samples/cylinder
5	36°	10	20	4
6	30°	12	24	4

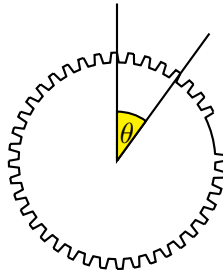


Figure 1: The flywheel angular velocity signal is generated by computing the time difference between two following teeth when the flywheel rotates. Two teeth are removed to keep track of the angular position of the flywheel.

To keep track of the angle of the flywheel in the vehicle control system, a crank counter variable is used. The crank counter is increased by one for each new sample of the flywheel angular velocity signal. As shown in Table 2, there are four samples of the flywheel angular velocity signal between two combustions. The firing order of the five cylinder engine is 1-2-4-5-3 and for the six cylinder engine 1-5-3-6-2-4. The crank counts associated to each cylinder for five and six cylinder engines are presented in Table 3 and follows the firing order of each engine. The crank counts have been selected by analyzing when the signal is affected by misfire which is discussed more in Section 5.1.1.

The speed signal is an estimation of the crankshaft angular velocity measured in revolutions per minute (rpm). The load signal measures the air mass in the cylinders per revolution,

Table 3: The crank counter values in the vehicle control system that are associated to each cylinder for five and six cylinder engines.

Cylinder	Crank counts	
	Five cylinder engine	Six cylinder engine
1	0, 1, 2, 3	1, 2, 3, 4
2	4, 5, 6, 7	17, 18, 19, 20
3	16, 17, 18, 19	9, 10, 11, 12
4	8, 9, 10, 11	21, 22, 23, 0
5	12, 13, 14, 15	5, 6, 7, 8
6	-	13, 14, 15, 16

measured in grams per revolution (r/rev). To handle dependencies of the flywheel angular velocity signal to different speeds and loads, the samples related to one cylinder, see Table 3, are associated to one of the operating points in Table 4. The operating points have been chosen the same as in the misfire detection algorithm used by Volvo Cars. Samples related to one combustion are classified to the closest, in the Euclidean sense, operating point given the speed and load signal at the last sample for the cylinder. The last sample is given at the last crank count for each cylinder, see Table 3. As an example for a six cylinder engine, samples of the flywheel angular velocity signal from cylinder 1 is classified to the closest operating point corresponding to the value of the speed and load at crank count 4.

Table 4: Data is categorized in 42 different operating points depending on the speed and load.

Load [g/rev]	Speed [rpm]					
	500	1000	1500	2000	2500	3000
0.3	*	*	*
0.4	*	*				⋮
0.6	⋮		⋮			
0.8						
1.2						
1.6	⋮				⋮	⋮
2.0	*	*

A catalytic converter warming flag in the vehicle control system is used to indicate when the ignition angle is chosen late in order to heat the catalytic converter during cold starts. Cold starts are known to be complicated when trying to detect misfires and the flag is used to identify when this occurs. Cold starts will be considered separately in the misfire detection algorithm using the catalytic converter warming flag.

3 Analysis of the flywheel angular velocity signal

Here, the flywheel angular velocity signal is analyzed and examples of how misfire and cold starts affect the flywheel are shown. The flywheel signal from a five cylinder engine is shown in Figure 2 where the samples related to one combustion of cylinder 3 are marked in the figure.

In Figure 3, two examples of the flywheel angular velocity signal from a five cylinder engine with misfire are shown. The effect of misfires are visible as a sudden increase in the measured time period. The increased time period is caused by the deceleration of the crankshaft and

driveline due to the missed torque from the combustion. Flywheel angular velocity signals with misfires from a six cylinder engine are shown in Figure 4. The same characteristic behavior is visible in the signals from a misfire as for the five cylinder engine. Comparing the two examples in Figure 3 and Figure 4, respectively, shows that the effects of a misfire to the flywheel signal varies depending on load and speed, which complicates misfire detection.

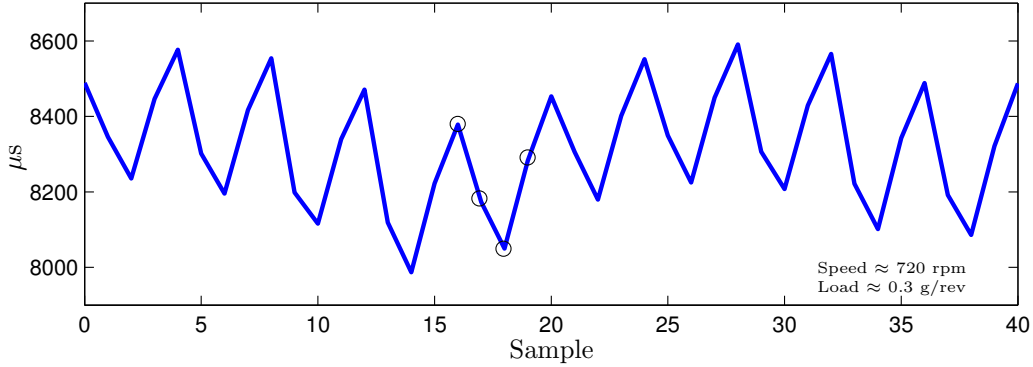


Figure 2: Example of angular velocity measurements at the flywheel from a five cylinder engine. Data related to one combustion from cylinder 3 is marked with circles.

As mentioned in the previous section, it is more difficult during cold starts to detect a misfire in the flywheel angular velocity signal, see Figure 5. The signal has a more stochastic nominal behavior and it is more difficult to distinguish an injected misfire from the other data because there are several jumps in the signal that are not related to any known misfire. Note that it is not known if these sudden increases in the signal are misfires or not.

The flywheel angular velocity signal depends on the speed and load which varies during a driving scenario. Figure 6 shows the flywheel angular velocity signal at one operating point, speed 1500 rpm and load 1.2 g/rev, for four of six cylinders. The blue curves represents the signal during the fault-free case and the red curves during the misfire case. The red curves are all within the variation of the blue curves and it is thus difficult to separate a misfire from fault-free data by just looking at the plots. Generally, in order to detect a misfire, the goal is to manipulate the data such that the fault-free data and misfire data are as separated as possible. The more the data from the two cases are separated, the easier it is to detect a misfire, using for example thresholding.

Comparing different methods to systematically improve misfire detectability requires a measure to quantify the separation between fault-free data and misfire data. To quantify the separation, the Kullback-Leibler divergence is used which is presented in the next section.

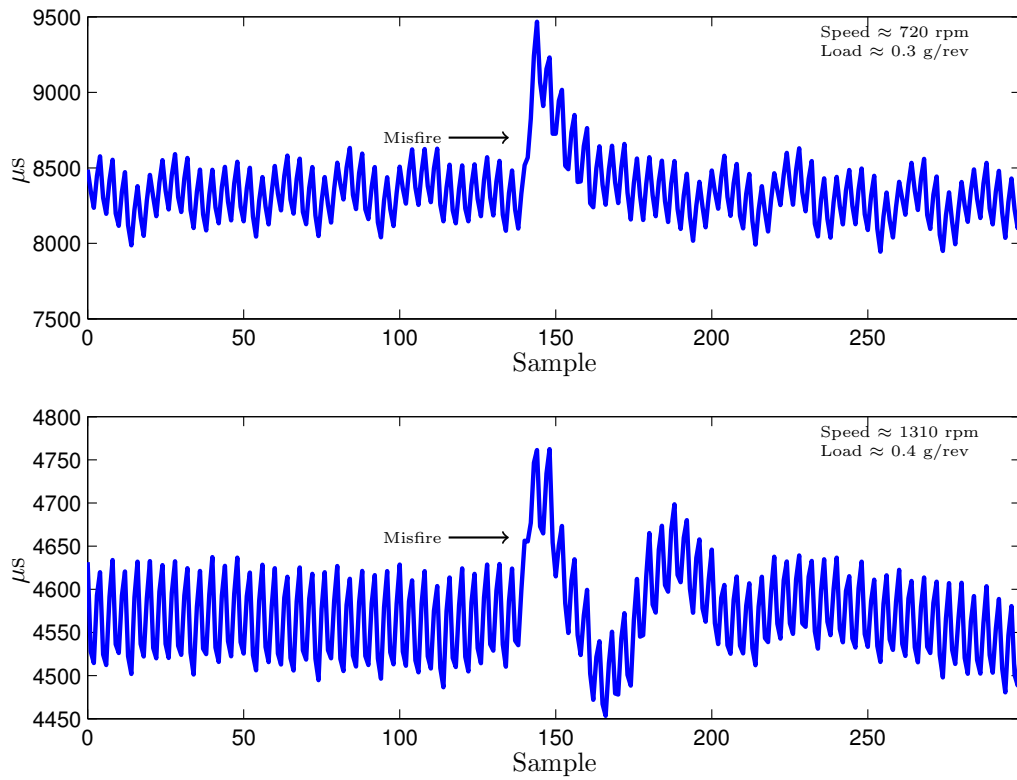


Figure 3: Examples of the flywheel angular velocity signal from a five cylinder engine. The signals contain misfires which are visible as increased measured time.

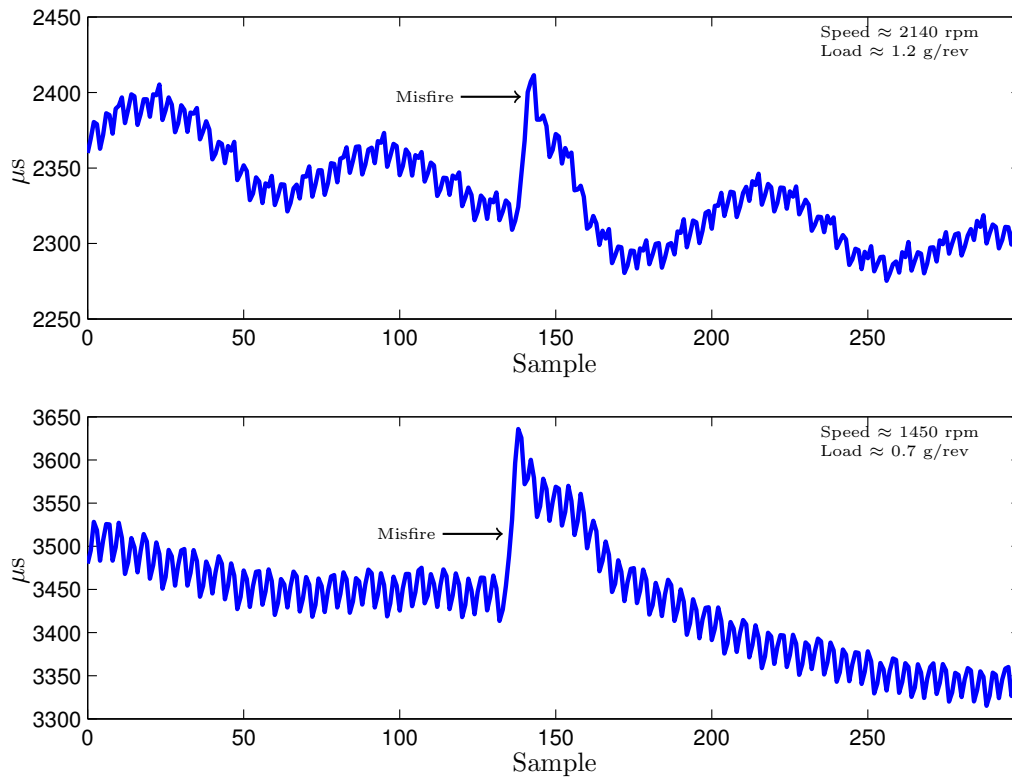


Figure 4: Examples of the flywheel angular velocity signal from a six cylinder engine. The signals contain misfires which are visible as increased measured time.

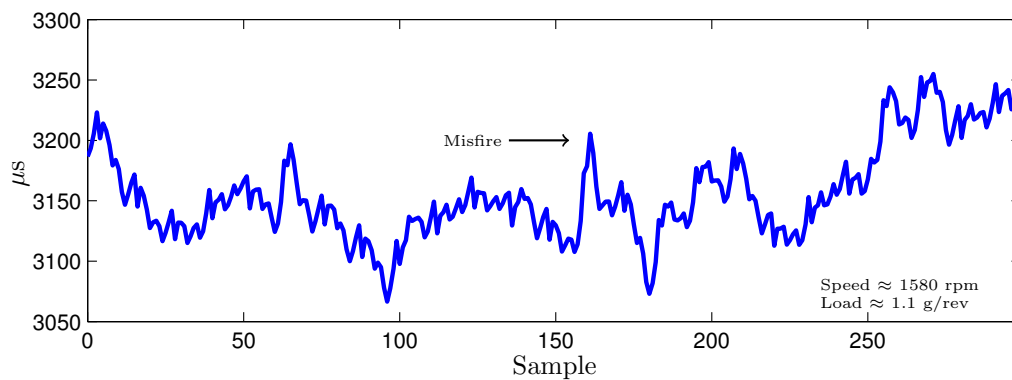


Figure 5: An example of the flywheel angular velocity signal from a six cylinder engine during cold start. Compared to signals in Figure 4, a misfire is more difficult to detect.

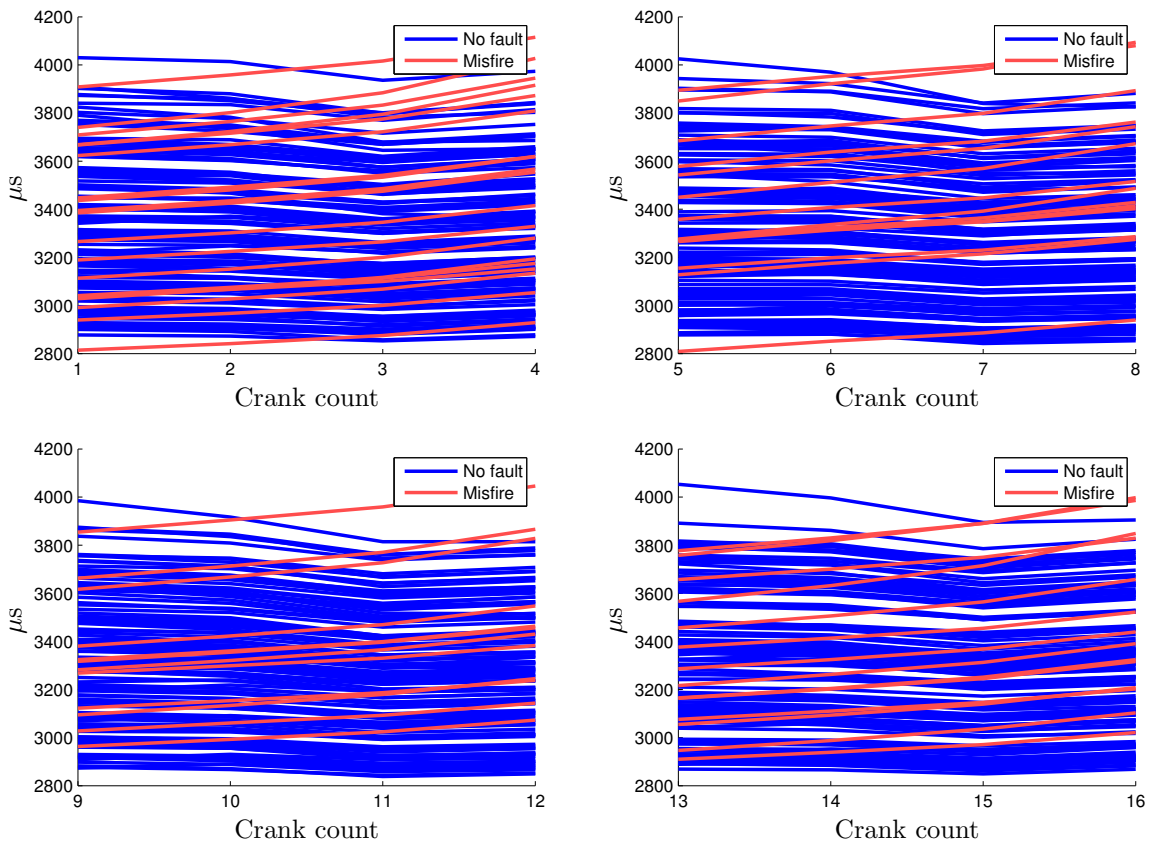


Figure 6: Flywheel angular velocity signal related to cylinder 1, 5, 3 and 6, see Table 3, during normal driving at operating point speed 1500 rpm and load 1.2 g/rev.

4 The Kullback-Leibler divergence

the Kullback-Leibler divergence is used here to quantify the misfire detectability performance of a signal or test quantity. The Kullback-Leibler divergence is suitable since it can be used to quantify the separation of the distributions of a given signal during the fault-free case and misfire case before constructing the misfire detection algorithm.

The Kullback-Leibler divergence [11] is a non-symmetric measure of the difference between two probability density functions, p_f and p_{nf} defined as

$$K(p_f||p_{nf}) = \int_{-\infty}^{\infty} p_f(x) \log \frac{p_f(x)}{p_{nf}(x)} dx \quad (1)$$

and is defined if:

- $p_{nf}(x) > 0$ for all x where $p_f(x) > 0$.
- If $p_f(x) = 0$ then $p_f(x) \log \frac{p_f(x)}{p_{nf}(x)} = 0$.

The Kullback-Leibler divergence is non-negative, i.e., $K(p_f||p_{nf}) \geq 0$ with equality if and only if $p_f = p_{nf}$, and asymmetric, i.e, in general $K(p_f||p_{nf}) \neq K(p_{nf}||p_f)$. A large value of (1) corresponds to that the distributions p_f and p_{nf} are well separated and it is easy to detect a misfire.

If p_{nf} is the distribution of the null hypothesis (no fault) and p_f is the distribution for the alternative hypothesis (misfire), then $K(p_f||p_{nf})$ can be interpreted as the expected log-likelihood ratio if p_f is the true hypothesis, see [5]. In [6], an alternative interpretation of the Kullback-Leibler divergence is: "How easy is it to distinguish if a sample is drawn from p_f (misfire) and not from p_{nf} (no fault)?" Thus, maximizing $K(p_f||p_{nf})$ would make it easier to detect a misfire. A value close to zero corresponds to the probability density functions, p_f and p_{nf} , being similar, i.e. it is hard to distinguish misfire data from fault-free data.

Computing (1), requires that the probability distributions of p_f and p_{nf} are known. Often, an analytical solution of (1) is not available. However, a numerical approximation can be made using training data. There are several approaches to compute approximations of the distributions p_f and p_{nf} if data are available. The distribution of the data can be approximated either by assuming a known parametric distribution, for example, the Gaussian distribution [3], or by using a non-parametric method such as kernel density estimators, see [1]. A kernel density estimator approximates a distribution by summing up a number of kernels, e.g., Gaussian distributions, centered around each sample of the data. A kernel density estimator for a one dimensional distribution, where each sample x_n of the signal is represented by a Gaussian probability density function with a mean value equal to the value of the sample, is

$$\hat{p}(x) = \frac{1}{N} \sum_{n=1}^N \frac{1}{(2\pi\sigma^2)^{1/2}} e^{-\frac{(x-x_n)^2}{2\sigma^2}} \quad (2)$$

where $\hat{p}(x)$ is the estimated probability density function, N is the length of the signal, and σ is the standard deviation of the Gaussian components, see [1]. If data from the misfire case and the fault-free case are clearly separated then the computation of (1) will depend only of the tails of the distribution p_{nf} since p_f is close to zero for fault-free data. The tails of the distribution are difficult to estimate since there are few data measured from the tails. When the distributions are well separated, parametric approximated distribution of the data can be used to model the tails.

If p_f and p_{nf} are Gaussian distributions with known means, μ_f and μ_{nf} , and co-variance matrices, Σ_f and Σ_{nf} , then (1) can be computed exactly, see [3]. For a one-dimensional Gaussian

distributed variable where $p_f \sim \mathcal{N}(\mu_f, \sigma_f^2)$ and $p_{nf} \sim \mathcal{N}(\mu_{nf}, \sigma_{nf}^2)$, the Kullback-Leibler divergence $K(p_f||p_{nf})$ is given by

$$K(p_f||p_{nf}) = \frac{1}{2} \left(\frac{\sigma_f^2}{\sigma_{nf}^2} + \frac{(\mu_{nf} - \mu_f)^2}{\sigma_{nf}^2} - \log \frac{\sigma_f^2}{\sigma_{nf}^2} - 1 \right). \quad (3)$$

Thus, by approximating the fault-free and misfire distributions of a signal as Gaussian distributions, the Kullback-Leibler divergence can be computed explicitly.

5 Torque estimation based on the angular velocity signal

As observed in Section 3, it is possible in most cases to manually identify a misfire in the flywheel angular velocity signal. However, when comparing several measurements at the same operating point, see Figure 6, it is difficult to select a fixed threshold to detect misfires while having a low probability of false alarms. Therefore, some additional signal processing is needed and here, the flywheel angular velocity signal is used to estimate the torque at the flywheel. Methods where cylinder torque is estimated in real-time for misfire detection can be found in, for example, [4] and [10]. In [10], the torque affecting the flywheel is described as

$$J\dot{\omega} = \sum_{i=1}^{n_{cyl}} (T_{c_i} + T_{p,i}) - T_{load} - T_{fr} \quad (4)$$

where J is the inertia of the flywheel, ω is the angular velocity of the flywheel, T_{c_i} is the torque from cylinder pressure at cylinder i , $T_{p,i}$ is the torque from piston mass at cylinder i , T_{load} is load torque and T_{fr} is friction. Each combustion results in a torque contribution T_{c_i} which is not present during a misfire.

The flywheel angular velocity signal $x[\theta]$ is sampled at a fixed angular interval $\Delta\theta$. The flywheel angular velocity signal $x[\theta]$ measures the time period Δt for a fixed angular interval $\Delta\theta$. An approximation of the flywheel angular velocity during the angular interval $\Delta\theta$ is computed as $\omega = \frac{d\theta}{dt} \approx \frac{\Delta\theta}{\Delta t} = \frac{\Delta\theta}{x[\theta]}$. Since the signal is angle synchronous, the relation (4) is written as

$$J \frac{d\omega}{d\theta} \underbrace{\frac{d\theta}{dt}}_{=\omega} = T \quad (5)$$

where $T = \sum_{i=1}^{n_{cyl}} (T_{c_i} + T_{p,i}) - T_{load} - T_{fr}$. The factor $\frac{d\omega}{d\theta}$ is approximated using Euler forward as

$$\frac{d\omega}{d\theta} \approx \frac{\frac{\Delta\theta}{x[\theta+\Delta\theta]} - \frac{\Delta\theta}{x[\theta]}}{\Delta\theta}. \quad (6)$$

A simple estimate of T is then given by

$$J \frac{\Delta\theta}{x[\theta]} \left(\frac{\frac{\Delta\theta}{x[\theta+\Delta\theta]} - \frac{\Delta\theta}{x[\theta]}}{\Delta\theta} \right) = J\Delta\theta z[\theta] (z[\theta + \Delta\theta] - z[\theta]) = T \quad (7)$$

where $z[\theta] = x^{-1}[\theta]$ and $J\Delta\theta$ is assumed constant and can be seen as a scaling factor.

Two examples of estimated torque using the flywheel angular velocity signal are shown in Figure 7. The flywheel angular velocity signals from a five cylinder engine that have been used are shown in Figure 3. A combustion in a cylinder results in an increase in torque but a misfire results in a smaller peak. Compared to the flywheel angular velocity signal, the estimated torque oscillates around zero, although the mean value is slightly positive. This is convenient

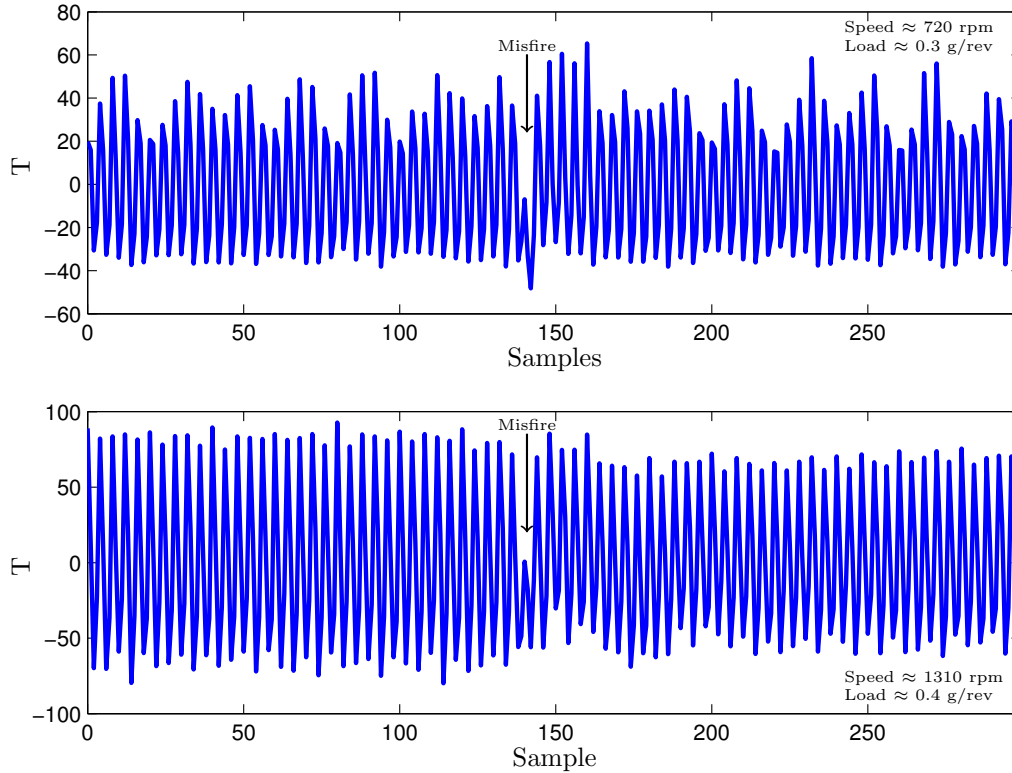


Figure 7: Examples of estimated torque from a five cylinder vehicle. The data contains misfires which are visible as smaller torque gain.

since there is no need of compensation in the signal for the variation in speed which will be shown in Section 5.1.

In Figure 8, two examples of estimated torque are shown using the flywheel angular velocity signal from the six cylinder engine shown in Figure 4. The estimated torque oscillates around zero but it shows a bigger torque drop from a misfire compared to Figure 7. The difference in shape between misfires in Figure 7 and Figure 8 are similar for different speeds and loads. The relative torque loss during misfire is bigger in general for the six cylinder engine case than for the five cylinder engine case.

Data from cold starts is only available from a six cylinder engine. Figure 9 shows the estimated torque from flywheel measurements during cold start where the corresponding flywheel angular velocity signal is shown in Figure 5. It is difficult to distinguish the misfire from other torque drops. However, there are some torque drops that are almost as low as the known misfire but it is not known if these drops are also caused by misfires.

To summarize this section, by estimating the torque at the flywheel, a misfire can be identified as a smaller torque gain from the misfiring cylinder. Also, since the estimated torque oscillates around zero, all data associated to the same operating point will have the same mean value. Thus, it is not necessary to compensate for varying speed when comparing data from each operating point to identify a misfire. The misfire detectability performance of using the estimated torque is further analyzed in Section 5.1

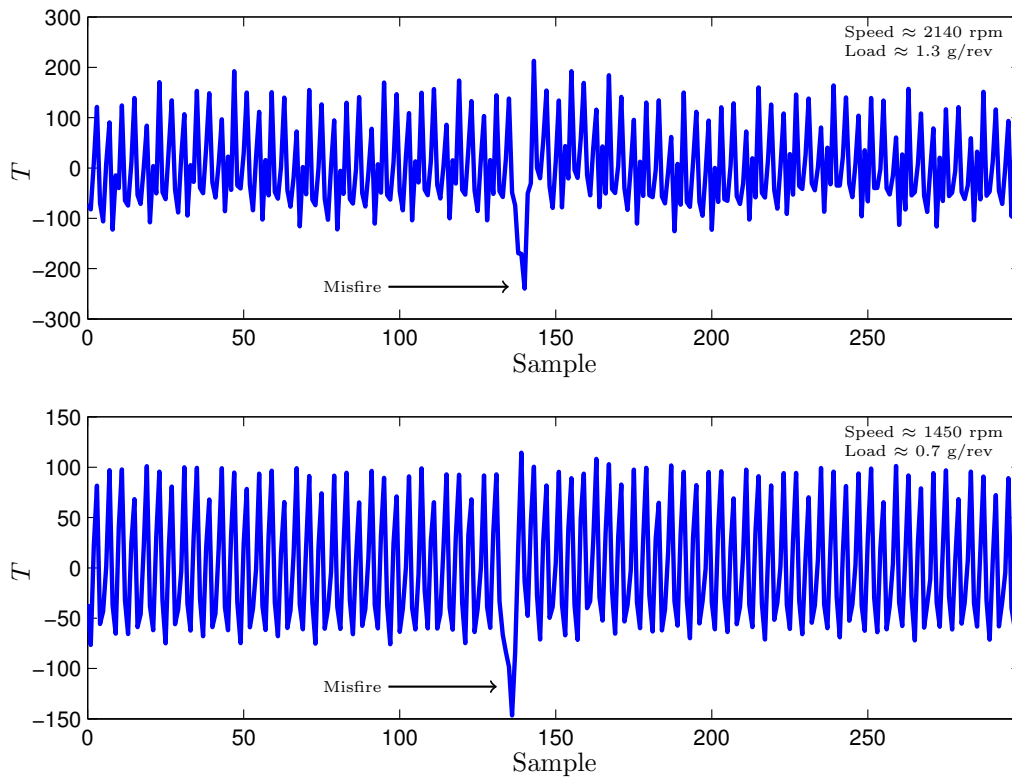


Figure 8: Examples of estimated torque from a six cylinder vehicle. The data contains misfires which are visible as smaller torque gain.

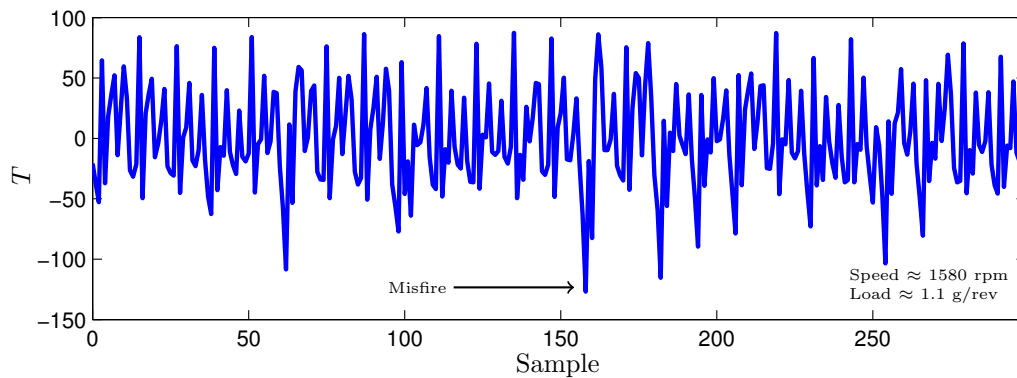


Figure 9: An example of estimated torque during cold start from a six cylinder vehicle. Compared to data in Figure 7, a misfire is more difficult to detect during cold starts.

5.1 Analyzing misfire detectability performance of estimated torque signal

In the previous section, the flywheel angular velocity signal is used to estimate the torque at the flywheel. An interesting question is how much performance is gained by using the estimated torque instead of the original flywheel signal. It is also interesting to analyze how the performance varies, depending on operating point and if it is during cold start or not. Here, the estimated torque based on fault-free data and misfire data is analyzed using the Kullback-Leibler divergence described in Section 4.

5.1.1 Signal distribution at one operating point

First, a comparison is made between torque estimation of fault-free data and misfire data for each cylinder separately at one operating point. An example of estimated torque for fault-free combustions and misfires for different cylinders at operating point speed 1500 rpm and load 1.2 g/rev are shown in Figure 10. Each plot shows the data from one cylinder where the upper left plot is cylinder 1, upper right plot is cylinder 5, lower left plot is cylinder 3 and lower right plot is cylinder 6. The plots show that the estimated torque clearly differs between normal behavior and misfire compared to the flywheel angular velocity signal shown in Figure 6. The difference between the distributions for each of the four cylinders in Figure 10 is largest at the second sample in each plot and smallest at the last sample.

Consider the upper left plot in Figure 10. The distribution of fault-free data and misfire data for each sample of cylinder 1 is plotted in Figure 11. The upper left plot is the distribution of the first sample of the combustion, the upper right is the second sample and so on. By comparing the four plots, it is clear that the distributions are separated the most at the second sample (upper right plot) and the least at the last sample (lower right plot) which is also shown in Figure 10.

Figure 12 shows the estimated torque during cold starts, at operating point speed 1500 rpm and load 1.2 g/rev. During cold starts, when the catalytic converter is heated, the difference between fault-free data and misfire data is smaller compared to the normal case which indicates that misfire detection is more difficult during cold starts compared to normal driving since the data is not as separated as in Figure 10. Note that some of the torque traces are similar to the torque during normal driving in Figure 10, which have maximum torque in the second sample. This might be caused by a latency in the catalytic converter warming flag.

A comparison of the sample distributions of cylinder 1 during cold start in the upper left plot in Figure 12 is shown in Figure 13. The distributions of fault-free data and misfire data are most separated in the last sample and the least in the first sample. A possible explanation for this is that during cold start the ignition angle is intentionally set later to heat the catalytic converter. Therefore, since the combustion occurs later, the effect of a combustion is visible later in the estimated torque compared to the results in Figure 11.

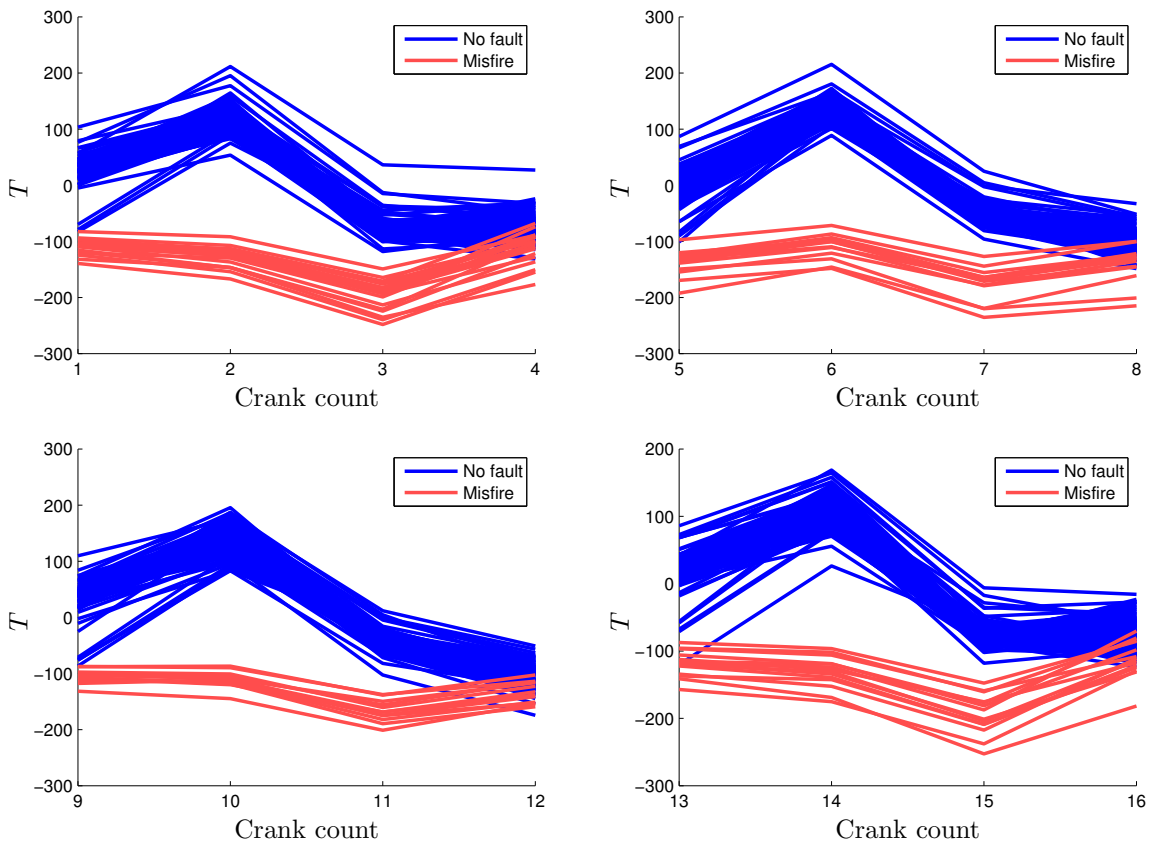


Figure 10: Estimated torque of cylinder 1, 5, 3, and 6 during normal driving at operating point speed 1500 rpm and load 1.2 g/rev.

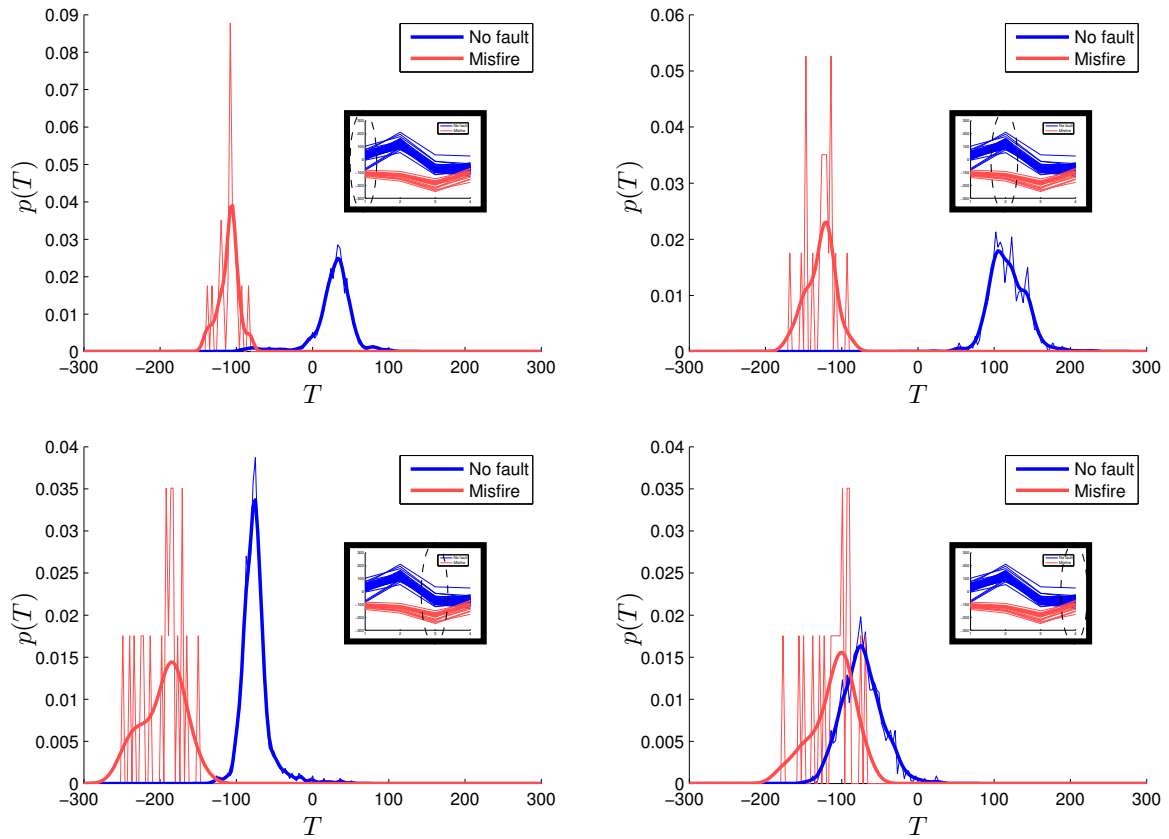


Figure 11: The distribution of the torque of cylinder 1, i.e., crank counts 1, 2, 3, and 4, during normal driving at operating point speed 1500 rpm and load 1.2 g/rev. A normalized histogram of the data and an approximation of each distribution using kernels is shown in each plot. The separation between torque from a fault-free combustion and a misfire is largest at the second sample and smallest at the last sample.

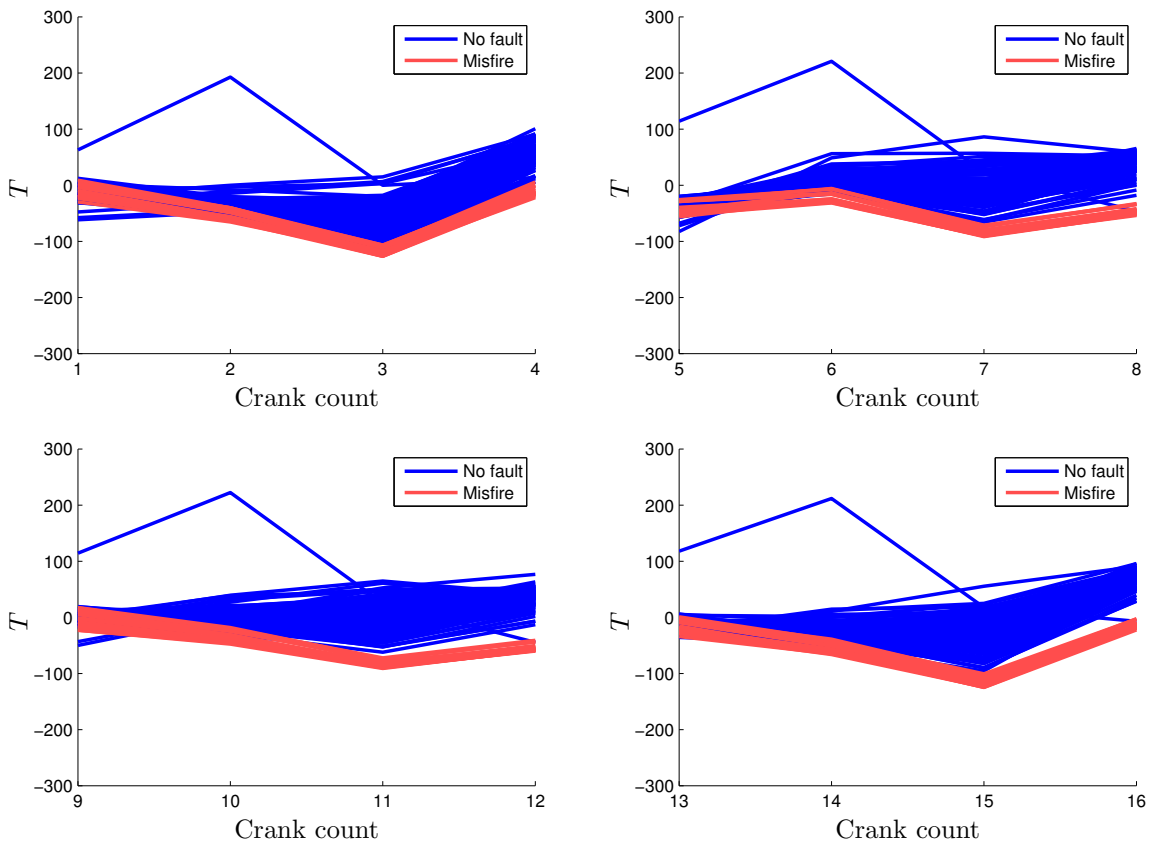


Figure 12: Estimated torque of cylinder 1, 5, 3, and 6 during cold start at operating point speed 1500 rpm and load 1.2 g/rev.

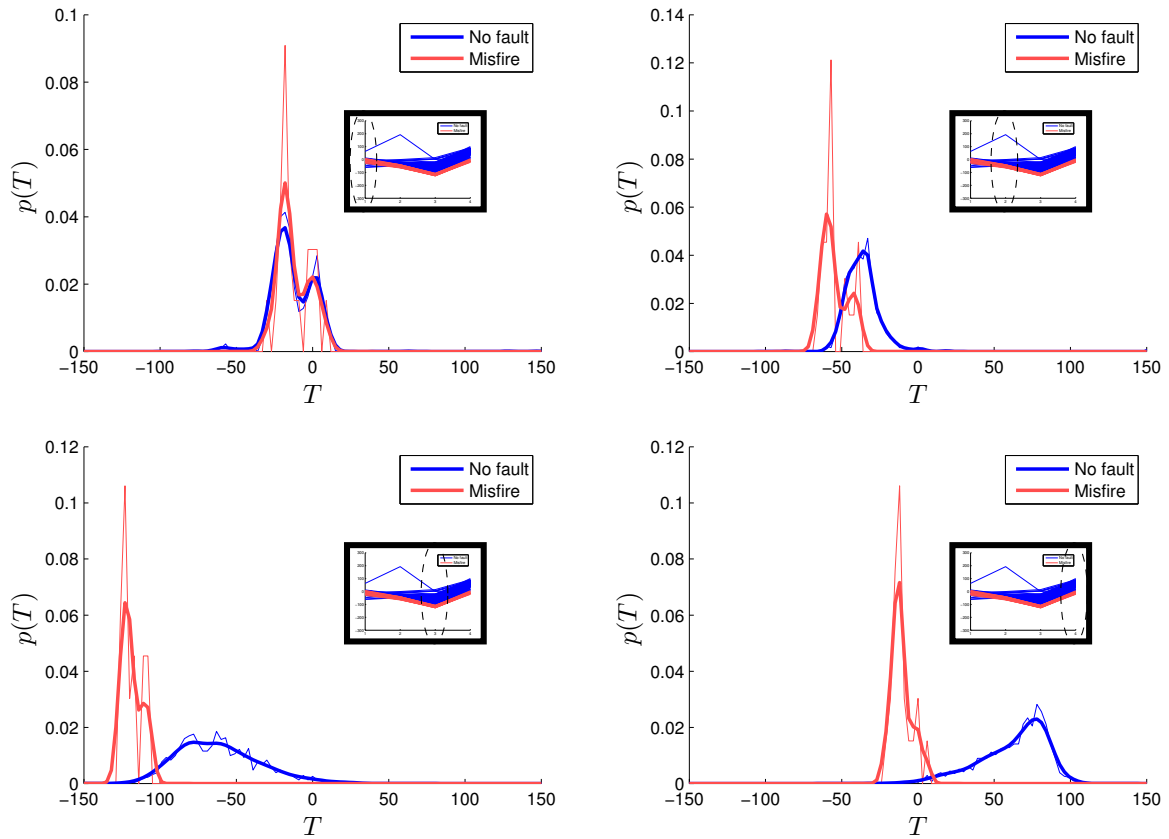


Figure 13: The distribution of the torque of cylinder 1, i.e., crank counts 1, 2, 3, and 4, during cold start at operating point speed 1500 rpm and load 1.2 g/rev. A normalized histogram of the data and an approximation of each distribution using kernels is shown in each plot. The separation between torque from fault-free combustion and a misfire is largest at the last sample and smallest at the first sample.

5.1.2 Analyzing signal distribution using the Kullback-Leibler divergence

Here, the Kullback-Leibler divergence is computed by approximating the fault-free data and misfire data as Gaussian distributed and using (3) to quantify the separation. The results are shown in Figure 14 for normal driving and in Figure 15 for cold starts. Comparing the normalized histograms of the data and the approximated Gaussian distributions shows that the approximation is not always representative of the data. However, a value of Kullback-Leibler divergence around 50 seems to correspond to well separated distributions but already around 20 the distributions are fairly separated such that few or no data from the fault-free case and misfire case are overlapping.

An interesting aspect is to analyze the gain by using the estimated torque instead of the original flywheel angular velocity signal. The computed Kullback-Leibler divergence in Figure 14 is compared to the Kullback-Leibler divergence of the corresponding flywheel angular velocity signal shown in the upper left plot in Figure 6. The distributions and computed Kullback-Leibler divergence are presented in Figure 16. The Kullback-Leibler divergence are all below 0.5 for all samples which is expected since the approximated distributions are similar. The differences in Kullback-Leibler divergence indicate that the estimated torque is more suitable to detect misfires compared to the original flywheel angular velocity signal.

Computing the Kullback-Leibler divergence, for example, for different cylinders or operating points, can be used to get an overview of how misfire detectability varies for different operating points. As an example, data from a city driving scenario in Gothenburg, Sweden, is used to compute the Kullback-Leibler divergence in Table 5. The Kullback-Leibler divergence is computed for fault-free data and misfire data for cylinder 1 and crank count 2 for different operating points. If data is not available from both the fault-free case and misfire case, the Kullback-Leibler divergence is not computed which is represented by an empty field. The computed Kullback-Leibler divergence is above 20 for all cases and increases for high speeds and high loads. The results indicate that it should be more difficult, in general, to detect a misfire at low loads and speeds around 1000 rpm compared to high speeds and loads.

Another example, using the same driving scenario, but estimated torque for cylinder 6 and crank count 14 is shown in Table 6. The Kullback-Leibler divergence is lower at low speeds and loads compared to Table 5 but increases for higher loads and speeds. The result from the two tables indicate that it should be in general more difficult to detect a misfire at low speed and load but easier at high speed and load.

In this section, the Kullback-Leibler divergence has been used to analyze the estimated torque to be used for misfire detection. The estimated torque is compared to the original flywheel angular velocity signal and the results show that the estimated torque is more suitable to use because it gives a higher value of Kullback-Leibler divergence. The Kullback-Leibler divergence is a useful tool to get an overview of how misfire detectability varies during a combustion and for different operating points. The analyzes have shown that, for example, depending on if it is during normal driving or a cold start, different samples during the combustion should be used to detect a misfire.

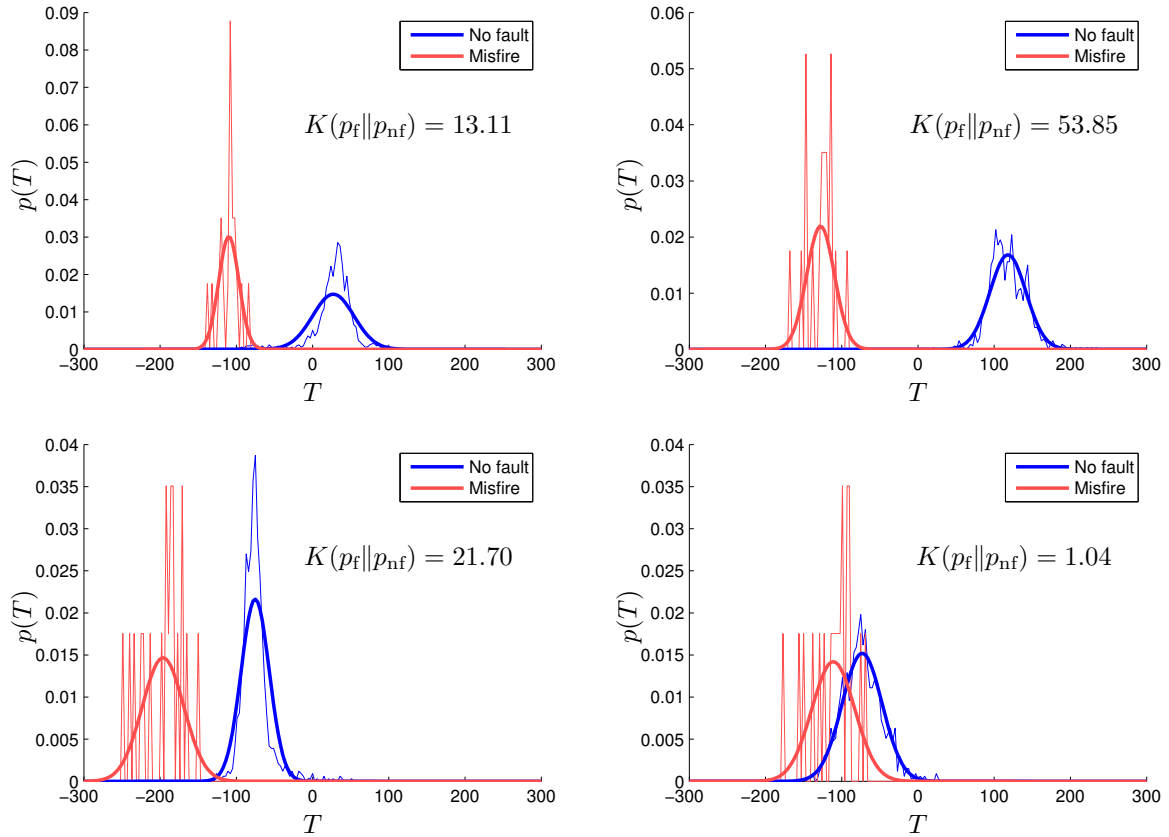


Figure 14: The distribution of the estimated torque of cylinder 1, i.e., crank counts 1, 2, 3, and 4, during normal driving at operating point speed 1500 rpm and load 1.2 g/rev. A normalized histogram of the data and an approximation of each distribution as a Gaussian is shown in each plot.

Table 5: Computed Kullback-Leibler divergence of Gaussian approximations of data from cylinder 1 (crank count 2) for different operating points.

Load [g/rev]	Speed [rpm]					
	500	1000	1500	2000	2500	3000
0.3		20.94	39.60			
0.4	51.95	20.30	28.21			
0.6	31.05	24.48	32.64	37.81		
0.8		27.54	44.22	38.11		
1.2			53.85	72.69		
1.6			94.76	96.45		
2.0				108.43		

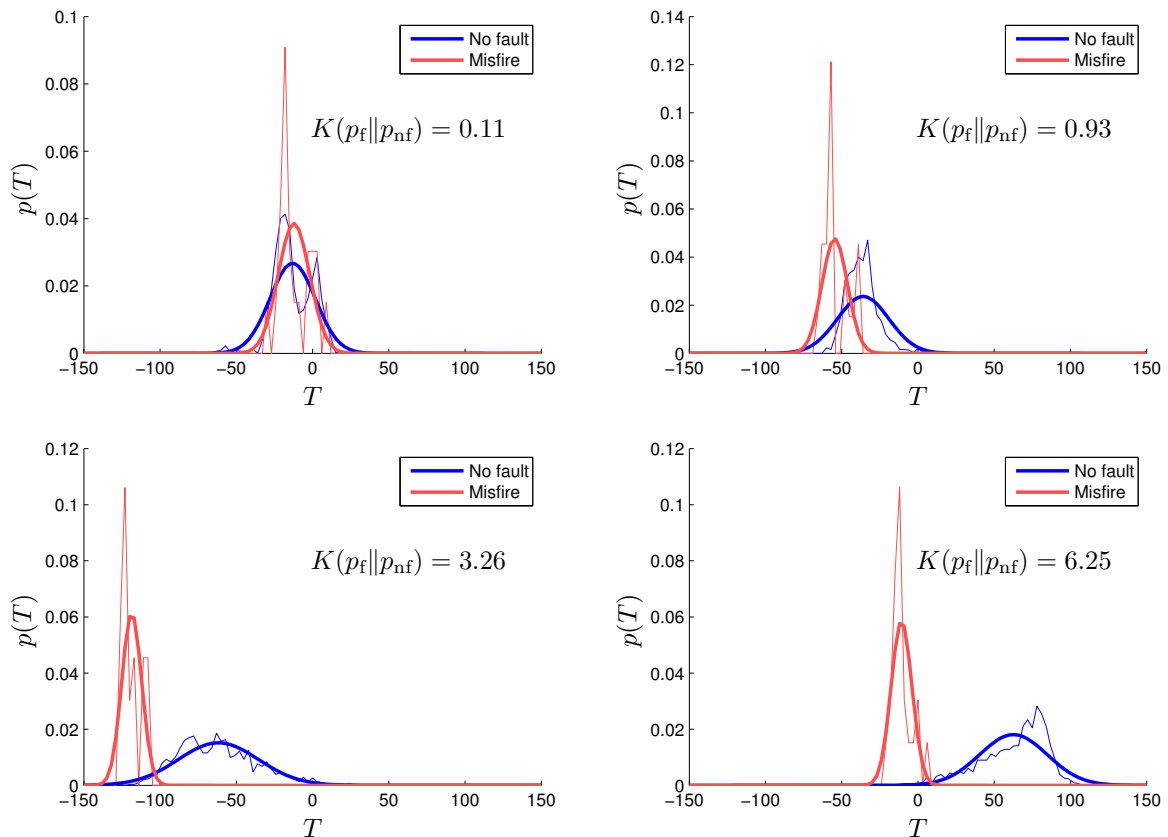


Figure 15: The distribution of the estimated torque of cylinder 1 during cold start at operating point speed 1500 rpm and load 1.2 g/rev. A normalized histogram of the data and an approximation of each distribution as a Gaussian is shown in each plot.

Table 6: Computed Kullback-Leibler divergence of Gaussian approximations of data from cylinder 6 (crank count 14) for different operating points.

Load [g/rev]	Speed [rpm]					
	500	1000	1500	2000	2500	3000
0.3		9.57	32.22			
0.4	33.17	12.73	23.20			
0.6	15.45	25.50	30.91	31.70		
0.8		31.07	46.54	32.34		
1.2			54.62	80.84		
1.6		27.44	69.84	124.20		
2.0			162.28	117.68	151.52	

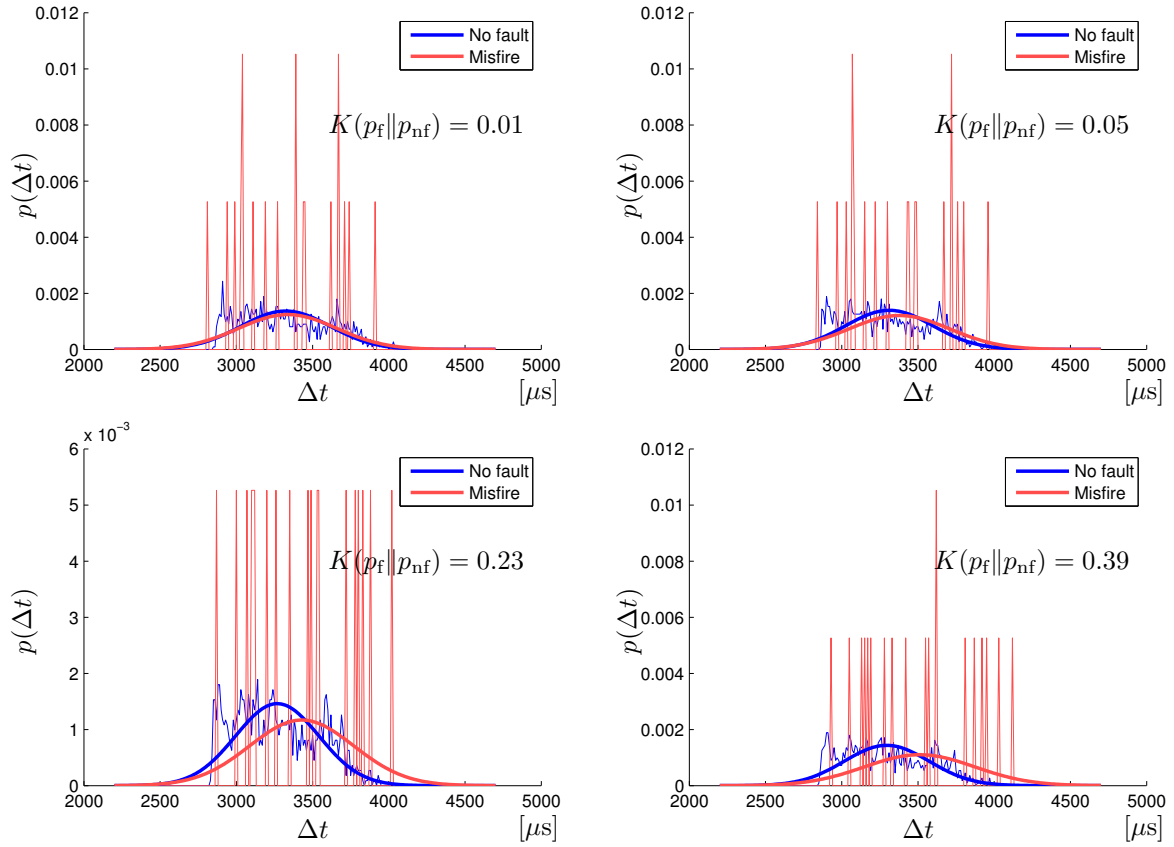


Figure 16: The distribution of the flywheel signal of cylinder 1 during normal driving at operating point speed 1500 rpm and load 1.2 g/rev. A normalized histogram of the data and an approximation of each distribution as a Gaussian is shown in each plot.

6 An algorithm for misfire detection

The flywheel angular velocity signal is used to estimate the torque at the flywheel. The Kullback-Leibler divergence has been used to show how misfire detectability performance depends on speed and load, and that fault-free data and misfire data are more separated at different samples depending on if it is during a cold start or not.

Here, a proposal for a misfire detection algorithm is presented based on the estimated torque. When designing the misfire detection algorithm, one goal has been to keep the solution simple in order to simplify parameter tuning. Another purpose is to let different steps in the design procedure be as independent from each other as possible. In that way, each step can be improved or replaced without the need of changing or removing other steps when tuning or running the algorithm.

6.1 Algorithm outline

Here, an outline of the misfire detection algorithm is presented. The algorithm can be summarized in the following steps.

1. Estimate the torque from the flywheel angular velocity signal.
2. Compute a test quantity using weights for data at different operating points.
3. Threshold the test quantity to detect a misfire.

The algorithm is designed such that all parameterization are automated, i.e., parameters and thresholds, are set automatically given training data. Step 1 of the algorithm has been described previously in Section 5. Step 2 is presented in Section 6.2 and step 3 is presented in Section 6.3.

6.2 Design of test quantity

Since the distribution of the estimated torque varies for different speeds and loads, the estimated torque from each operating point is considered separately. Also, estimated torque from normal driving and from cold starts are considered separately.

Step 1 of the algorithm described in Section 6.1, is to estimate the torque at the flywheel from the flywheel angular velocity signal. The torque at the flywheel is estimated using (7). The estimated torque from one combustion is classified to the closest operating point, see Table 4, given the value of the speed and load variables from the vehicle control system at the last sample of the combustion.

In this report, an adaptive compensation of flywheel manufacturing errors has not been considered. The difference in distribution of estimated torque for different cylinders at the same operating point is probably partly caused by flywheel errors. If available, a flywheel error compensation can be included in the first step of the algorithm. Here, to handle the errors which affect the torque estimation, each cylinder is considered separately. For the given number of operating points based on speed and load, the number of cylinders, and the catalytic converter heating flag will result, in total of $42 * 5 * 2 = 420$, modes to be parameterized for a five cylinder engine. However, if an adaptation of the estimated torque is included, such that the distribution is compensated for all cylinders, the number of modes would reduce by a factor five to 84.

In Section 5.1.2, the separation between the distributions of fault-free data and misfire data have been compared for each sample separately. One simple approach to design a test quantity is to take the one data point where the separation between the distributions are maximally separated. However as shown in Section 5.1.2, a misfire is more or less visible in all samples related to the cylinder depending on how much the misfire and fault-free distributions

are separated. Instead of looking at each sample independently, the different samples can be weighted together such that a good misfire detectability performance is achieved. In Figure 17, the three last samples of the estimated torque, denoted T_2 , T_3 , and T_4 , shown in Figure 11 and Figure 13, are plotted in a three dimensional space. The three dimensional distributions of estimated torque during cold starts and normal driving are marked in the figure. The two cases are clearly distinct from each other, thus requiring different weights to detect misfires for each case.

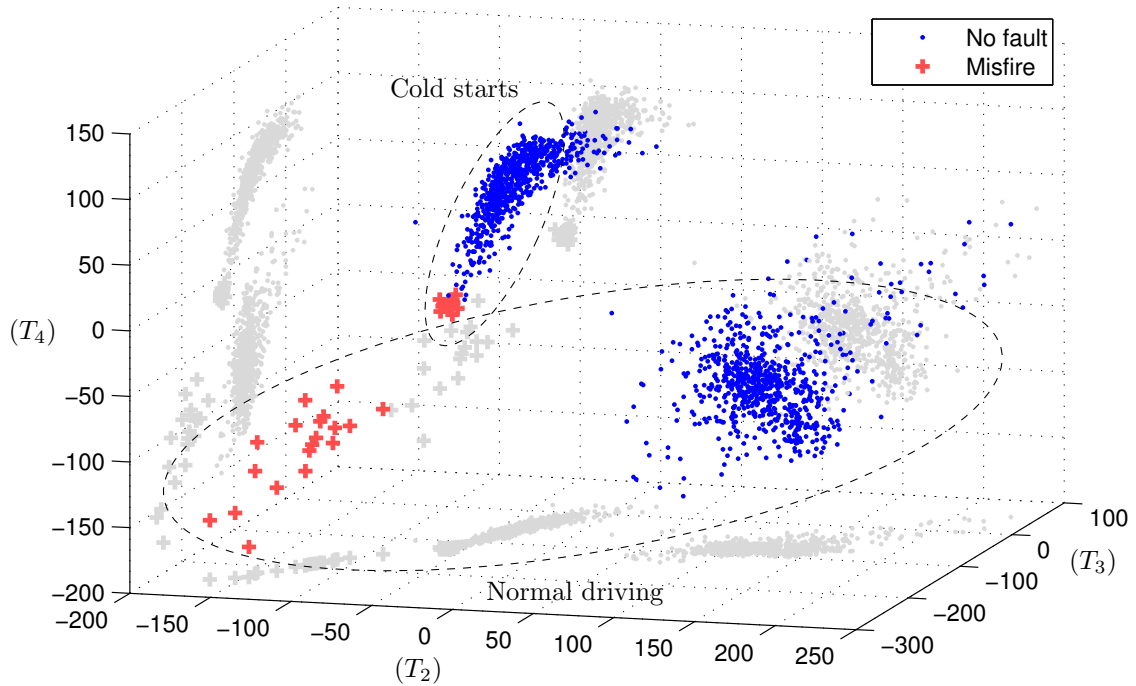


Figure 17: Estimated torque for three of the four samples shown in Figure 11 and Figure 13. The estimated torque at crank count 2 is T_2 , the estimated torque at crank count 3 is T_3 , and the estimated torque at crank count 4 is T_4 .

There are many ways to utilize all samples from one combustion to find a test quantity where the distribution of fault-free data and misfire data are as separated as possible, e.g., data-driven methods, see [1]. An implementation of a misfire detection algorithm where computational power is limited, requires that the complexity of the misfire detection performed on-line should be as low as possible. To reduce complexity of the misfire detection algorithm, a linear weighting function is applied when designing the test quantity. During each combustion, the torque is estimated four times, $\{T_1, T_2, T_3, T_4\}$. A test quantity y for detecting misfires is designed using linear weights as

$$y = \sum_{i=1}^4 \alpha_i T_i \quad (8)$$

where α_i is the weight for the estimated torque T_i and $\|\alpha\|^2 = 1$. The weights $\{\alpha_1, \alpha_2, \alpha_3, \alpha_4\}$ are chosen such that the value of y during the fault-free case and during misfire are as separated as possible.

Finding the weights $\alpha = (\alpha_1, \alpha_2, \alpha_3, \alpha_4)$ can be formulated as an optimization problem

$$\begin{aligned} & \max_{\alpha} M(p_f, p_{nf}; \alpha) \\ & \text{s.t. } \|\alpha\| = 1 \end{aligned} \quad (9)$$

where $M(p_f, p_{nf}; \alpha)$ is a measure of the separation between the distributions of y for fault-free data p_{nf} and misfire data p_f for a given α . Since p_{nf} and p_f are unknown, the probability density functions are approximated using training data.

As an example to visualize the weights of the vector α , the direction of one vector α is plotted together with the training data. The training data in Figure 17 is separated in two sets shown in Figure 18, the upper plot contains data from normal driving and the lower plot contains data from cold starts since these two cases have clearly separated distributions. The outlier in the cold start data is the same as the outlier in Figure 12. As an example, the solid lines represents the vector of the weights α for each data set which are parallel to the direction in which the distributions are separated.

In the upper plot in Figure 18 a threshold, exemplified by a dashed line, can easily be chosen such that a classification can be made with low risk of missed detection or false alarms. In the lower plot, the distributions are more overlapped and it is not possible by linear weights α to find a threshold which completely separates the data from the two cases. The weights α are different for normal driving and cold starts. Note that the weights α are largest for samples where the distributions were separated the most in Figure 14 and Figure 15, for example α_2 and α_3 for normal driving data and α_3 and α_4 for cold start data.

Here follows two proposed measures $M(p_f, p_{nf}; \alpha)$ that can be used to find a suitable α .

Maximizing the Kullback-Leibler divergence

One choice of $M(p_f, p_{nf}; \alpha)$ could be to find weights α which maximizes the Kullback-Leibler divergence, i.e,

$$M(p_f, p_{nf}; \alpha) = K(p_f(\alpha) \| p_{nf}(\alpha)) \quad (10)$$

where $p_f(\alpha)$ and $p_{nf}(\alpha)$ represents the distributions of y for the misfire case and fault-free case respectively for the given weights α . By maximizing (10), the distributions are optimally separated given the definition of Kullback-Leibler divergence.

As an example, optimized weights α which maximizes the Kullback-Leibler divergence for cylinder 1 at different operating points are presented in Figure 19. The weights are optimized given data from a driving scenario in Gothenburg. Each plot represents one sample for the different operating points. The Kullback-Leibler divergence is computed by estimating the distributions $p_f(\alpha)$ and $p_{nf}(\alpha)$ using the kernel density estimator in (2).

Comparing the weights for each sample in Figure 19 shows that the weights for each sample varies for different operating points. The second sample (crank count 2) has a high weight for most of the operating points while the other three samples (crank counts 1, 3, and 4) varies around zero. The misfire detection algorithm is evaluated when optimizing the weights using the Kullback-Leibler divergence in the next section.

Maximizing the gap between distributions

Let y_{nf} denote the vector of all fault-free data of the test quantity and y_f all misfire data.

$$M(p_f, p_{nf}; \alpha) = \begin{cases} \min(y_{nf}) - \max(y_f) & \text{if } \min(y_{nf}) > \max(y_f) \\ \min(y_f) - \max(y_{nf}) & \text{if } \max(y_{nf}) < \min(y_f) \end{cases} \quad (11)$$

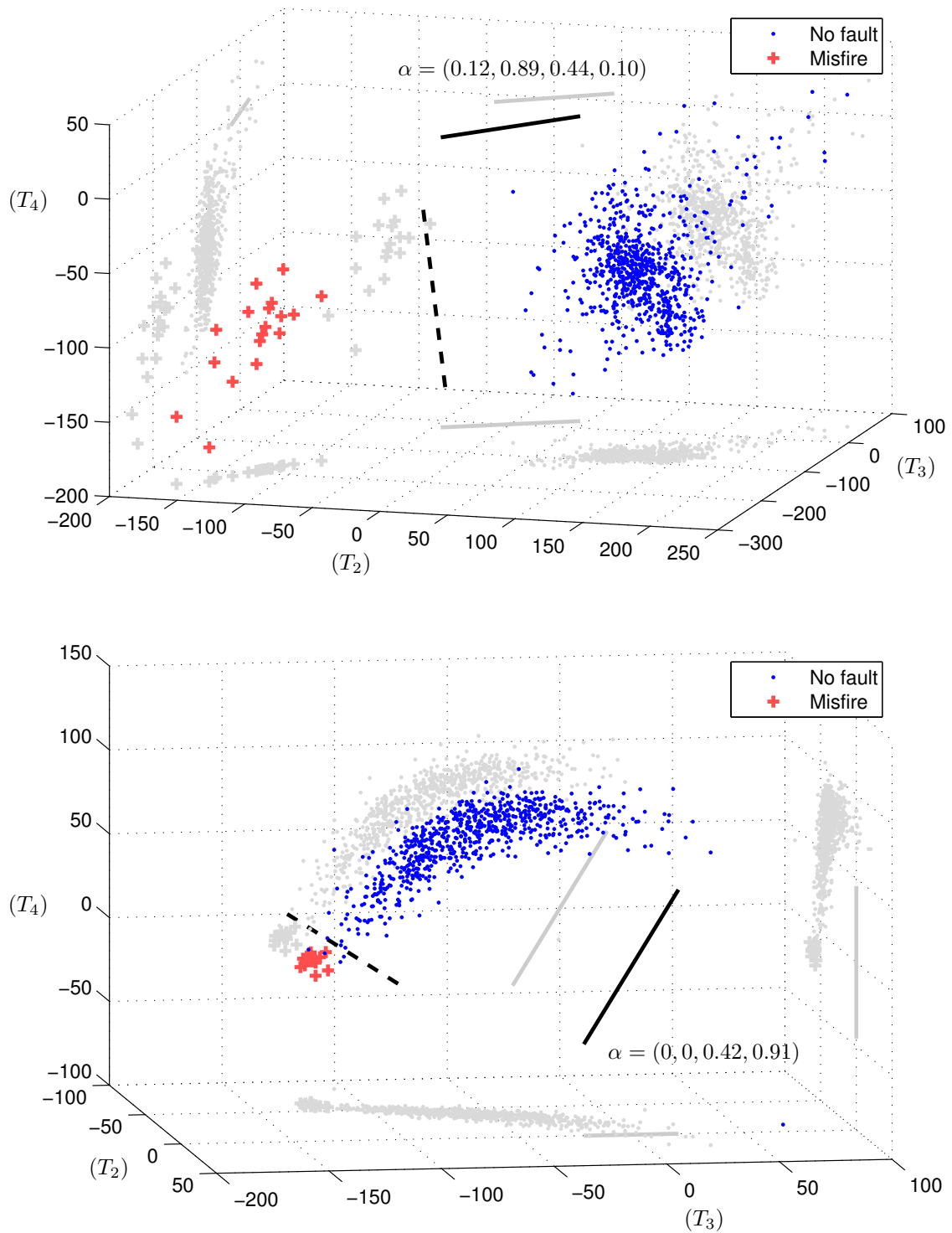


Figure 18: The data in Figure 17 is separated in normal driving, the upper plot, and cold starts, the lower plot. The solid lines represent the weights α such that the distributions of fault-free data and misfire data are well separated. Examples of thresholds to separate fault-free data and misfire data are shown as dashed lines.

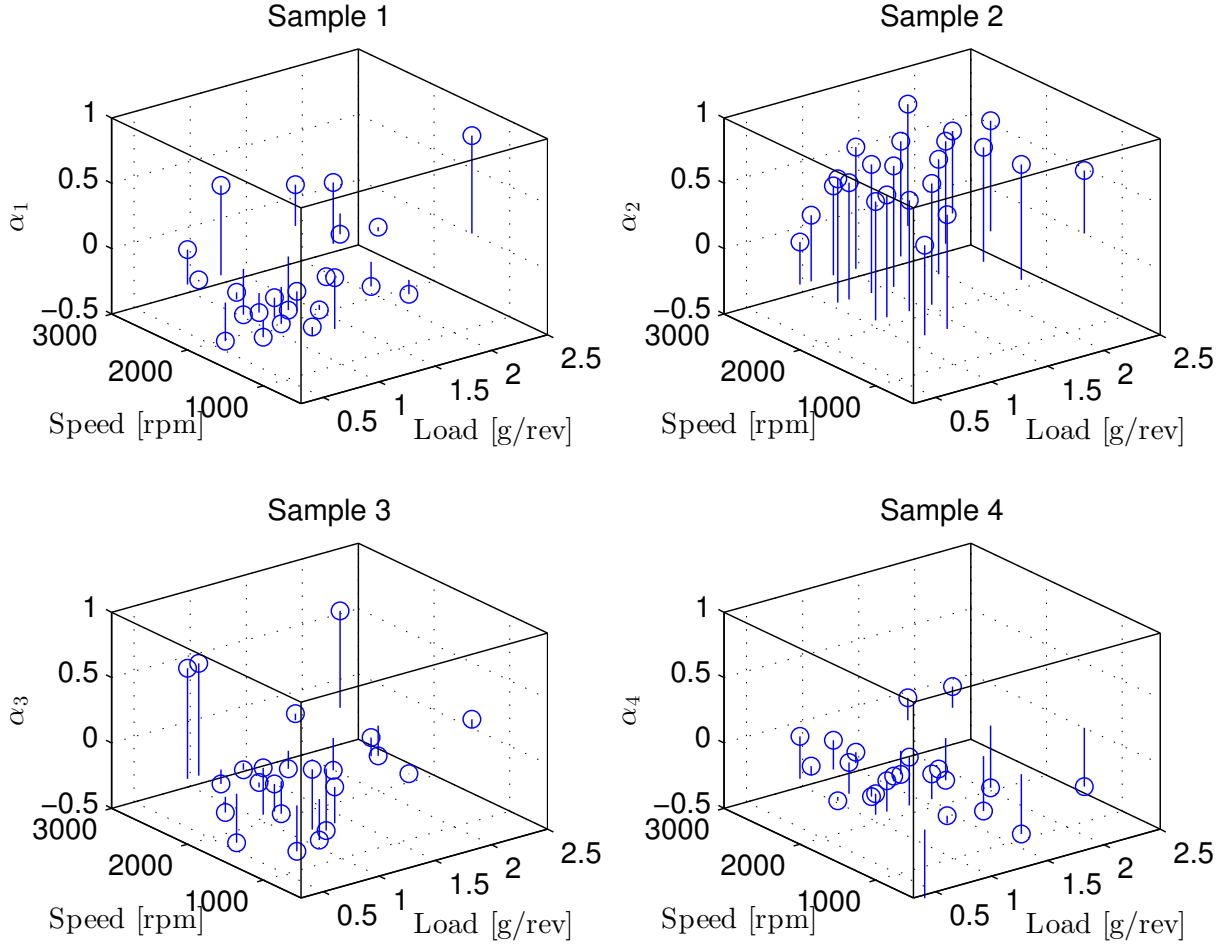


Figure 19: Optimized weights α for samples from cylinder 1 which maximizes the Kullback-Leibler divergence from the misfire distribution to the fault-free distribution.

Maximizing the gap is also applied in support vector machines to find planes which separate different classes given training data, see [1]. Note that maximizing the gap is sensitive to outliers since it only considers the closest data points of the two distributions.

In Figure 20, optimized weights are shown which maximizes the gap between distributions of the fault-free data and misfire data for cylinder 1 at different operating points. The data used here is the same data as in Figure 19. Comparing the optimized weights in Figure 20 and Figure 19, shows that the weights appear to vary less when maximizing the gap compared to maximizing the Kullback-Leibler divergence. The misfire detection algorithm is evaluated when optimizing the weights such that the gap is maximized in the next section.

6.3 Thresholding

The simplest and most common approach to detect a change in a test quantity y is the use of a fixed threshold J such that

$$\begin{aligned} y > J & \text{ concludes no misfire} \\ y \leq J & \text{ concludes misfire.} \end{aligned}$$

Depending on the fault-free and misfire distributions of the test quantity, the threshold are chosen to balance the risk of missed detections and false alarms.

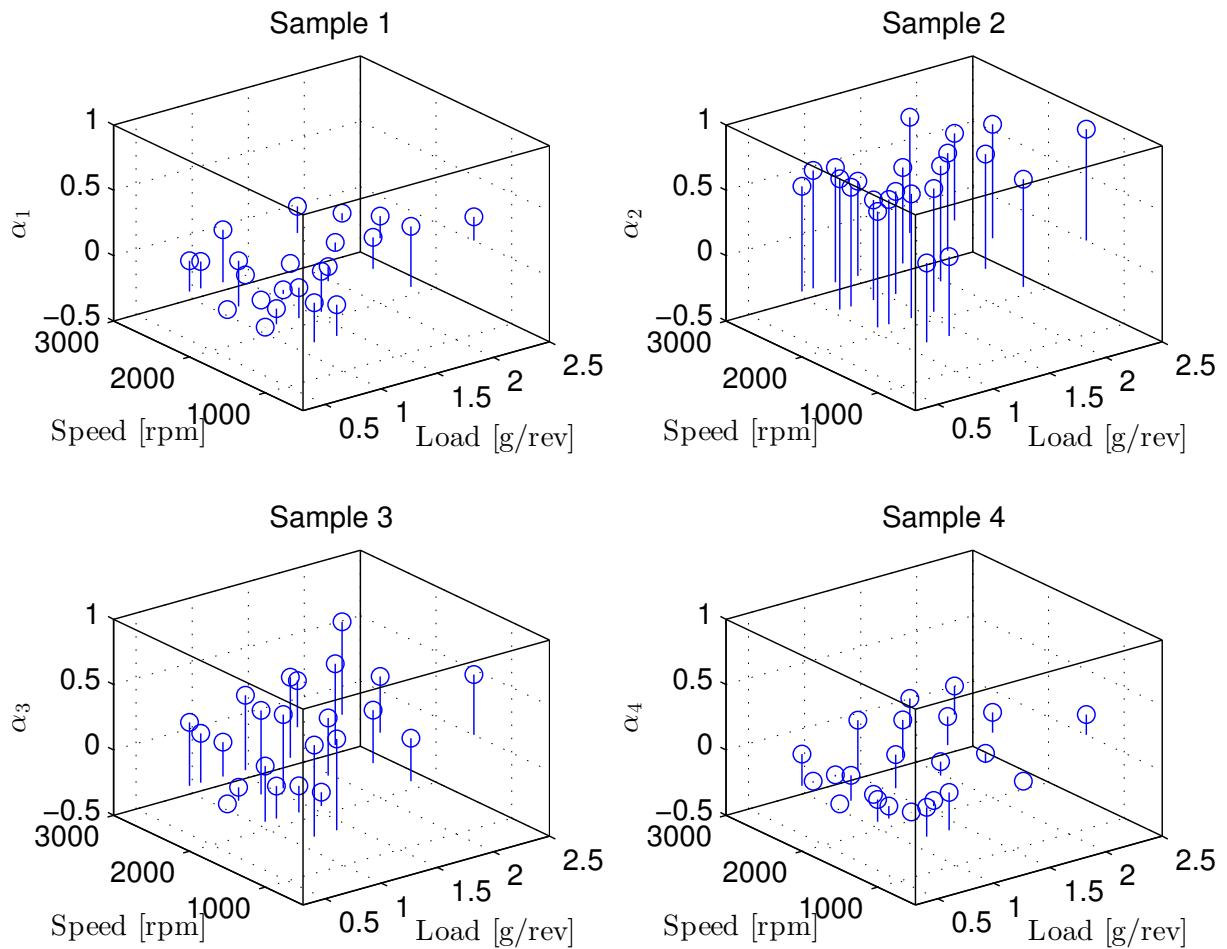


Figure 20: Optimized weights α for samples from cylinder 1 which maximizes the gap between the fault-free and misfire distributions.

By using training data to approximate the distributions of fault-free data and misfire data, thresholds can be automatically selected to balance the required performances.

7 Evaluation of the misfire detection algorithm

The purpose of this evaluation is to see how well separated misfire data and fault-free data are for a designed test quantity. One goal is to see if it is possible to select thresholds such that all misfires can be detected with few false alarms.

A test quantity is designed by estimating the torque from the flywheel angular velocity signal using (7). By using the speed and load variables, the crank counter, and the catalyst warming flag, from the vehicle control system, the estimated torque is associated to a specific operating point, cylinder, and if it is during a cold start or not. For each case, a vector α in (8) which solves (9), has been optimized using Matlab and an interior-point search algorithm, see [2]. The distributions of the test quantity are estimated using a set of training data. Two versions of the misfire detection algorithm are evaluated using two different sets of vectors α . The first version has weights α such that the Kullback-Leibler divergence (10) is maximized and the second version has weights α such that the gap between fault-free data and misfire data (11) is maximized. Note that a misfire is detected by analyzing samples associated to one specific cylinder. Thus, identification of the misfiring cylinder is obtained automatically.

Constant thresholds, which decides when a misfire is detected, are selected for each operating point, cylinder, and state of the catalyst warming flag. Parameterization of the algorithm is made given a set of training data in the following order.

1. Estimate torque using (7).
2. Compute vectors α for the test quantity y in (8) for each operating point using (9).
3. Compute thresholds which fulfills required probabilities for false alarm and missed detection.

All parameterization is performed automatically using training data and the only necessary manual tuning is to choose probabilities for false alarm and missed detection.

To be sure that there is a sufficiently large set of training data for all operating points in the validation data, the validation data is included in the training data. Thresholds are chosen just above the highest value of the test quantity for any misfire in the training data, i.e., all misfires in the training data are detected. This choice of the thresholds is used to analyze how separated the distributions of misfire data and fault-free data are, by looking at the number of false alarms. If the number of false alarms is high when all misfires are detected then it is not possible to reduce the number of false alarms without increasing the number of missed detections.

For a six cylinder engine, the misfire detection algorithms are evaluated using one normal driving scenario and three cold start scenarios. The two versions of the misfire detection algorithm are compared to Volvo's misfire detection algorithm which is used as a reference where the number of detected true misfires, false alarms and missed detections are compared. Note that Volvo's misfire detection algorithm is the implemented algorithm for the vehicle and is not tuned using the training data as for the other algorithms. The results for each scenario are shown in Tables 7-10. Table 7 summarizes the result from the normal driving scenario. The two versions of the algorithm have no false alarms and an example of the test quantities and thresholds are shown in Figure 21 and Figure 22 respectively. In the cold starts scenarios, there are some false alarms for both versions of the algorithm which is inevitable since the fault-free data and misfire data are overlapping, as shown in Figure 18, and can not be completely separated. The results in Tables 8-10 show that both maximizing the Kullback-Leibler divergence and maximizing the gap give a better performance than the reference algorithm in almost all

cases. However, maximizing the Kullback-Leibler divergence seems to give a slightly better performance compared to maximizing the gap.

Examples of the test quantities and thresholds when maximizing the Kullback-Leibler divergence and maximizing the gap are shown in Figure 21 and Figure 22 respectively. The figures show how the threshold varies depending on speed, load, and cylinder, where a large jump corresponds to a change in operating point and the small variations are different cylinders. The two dips of the test quantity are the result of misfires. Given the data in both Figure 21 and Figure 22, the thresholds can be chosen higher without significantly increasing the risk of false alarms. This is also visible when looking at the separation between the distributions of the test quantities shown in Figure 23 and Figure 24 which gives examples of the distributions for two operating points and two cylinders. The thin lines are normalized histograms of the fault-free data and misfire data and the thick lines are approximated distributions using (2). The test quantities during cold start when maximizing the Kullback-Leibler divergence and maximizing the gap are shown in Figure 25 and Figure 26 respectively. The distributions of the test quantities are shown in Figure 27 and Figure 28. Misfires during cold starts are most difficult to detect at the operating point load 1.2 g/rev and speed 1500 rpm but the distributions are better separated compared to looking at each sample individually, see Figure 12.

The evaluation of the two versions of the misfire detection algorithm for a five cylinder engine is shown in Table 11 and Table 12. The algorithms are evaluated using two driving scenarios. No cold start scenarios were available for the five cylinder engine and the performance in this case has not been evaluated. The number of false alarms for the two versions of the misfire detection algorithm are fewer compared to the reference algorithm.

The evaluations show some promising results that the misfire detection algorithms proposed in this work are able to detect all misfires while having few false alarms. Two approaches to choose the weights α are compared and they seem to give similar performance considering number of false alarms when detecting all misfires.

Table 7: Results for a six cylinder engine from a normal driving scenario. The number of combustions during the scenario is 60356.

	Max. K-L	Max. gap	Ref.
Detected true misfires	1 021	1 021	871
Missed detections	0	0	150
False alarms	0	0	58

Table 8: Results for a six cylinder engine from a cold start scenario at 7°C. The number of combustions during the scenario is 6137.

	Max. K-L	Max. gap	Ref.
Detected true misfires	127	127	61
Missed detections	0	0	66
False alarms	9	13	19

Table 9: Results for a six cylinder engine from a cold start scenario at 21°C. The number of combustions during the scenario is 3962.

	Max. K-L	Max. gap	Ref.
Detected true misfires	82	82	14
Missed detections	0	0	68
False alarms	13	19	16

Table 10: Results for a six cylinder engine from a cold start scenario at 25°C . The number of combustions during the scenario is 3251.

	Max. K-L	Max. gap	Ref.
Detected true misfires	66	66	10
Missed detections	0	0	56
False alarms	7	6	11

Table 11: Results for a five cylinder engine from a normal driving scenario. The number of combustions during the scenario is 122283.

	Max. K-L	Max. gap	Ref.
Detected true misfires	953	953	945
Missed detections	0	0	8
False alarms	9	24	78

Table 12: Results for a five cylinder engine from a normal driving scenario. The number of combustions during the scenario is 10339.

	Max. K-L	Max. gap	Ref.
Detected true misfires	2	2	2
Missed detections	0	0	0
False alarms	21	18	23

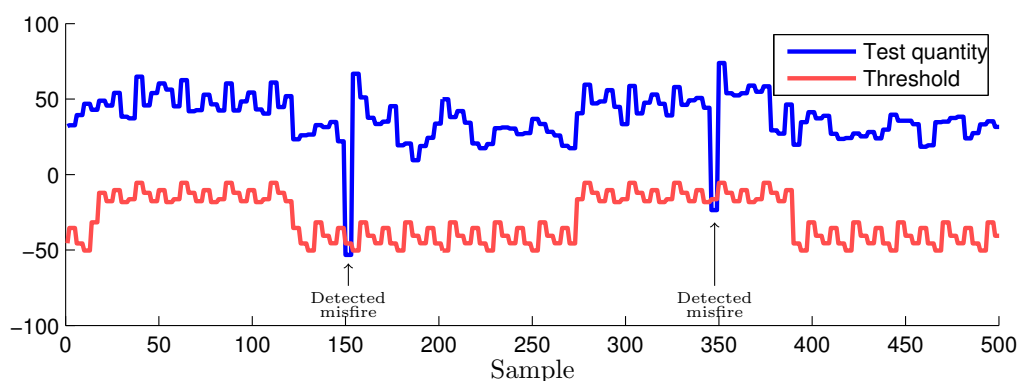


Figure 21: An example of the test quantity and threshold, when maximizing the Kullback-Leibler divergence, for a six cylinder engine during normal driving. The threshold variations depends on operating point and cylinder.

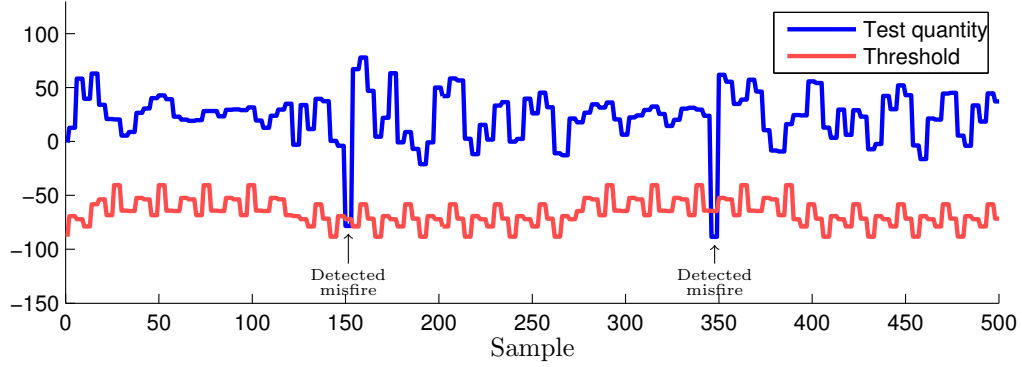


Figure 22: An example of the test quantity and threshold, when maximizing the gap, for a six cylinder engine during normal driving. The threshold variations depends on operating point and cylinder.

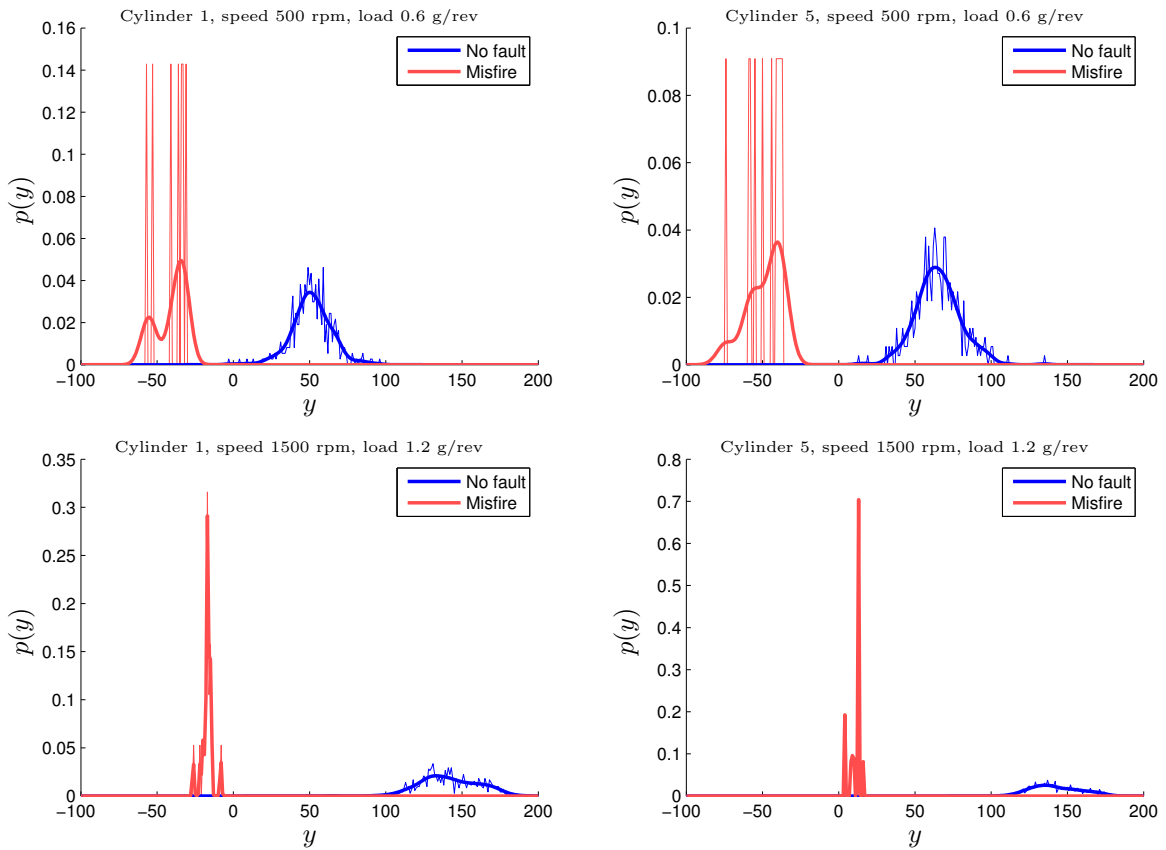


Figure 23: The distribution of the test quantity for different loads and speeds when maximizing the Kullback-Leibler divergence.

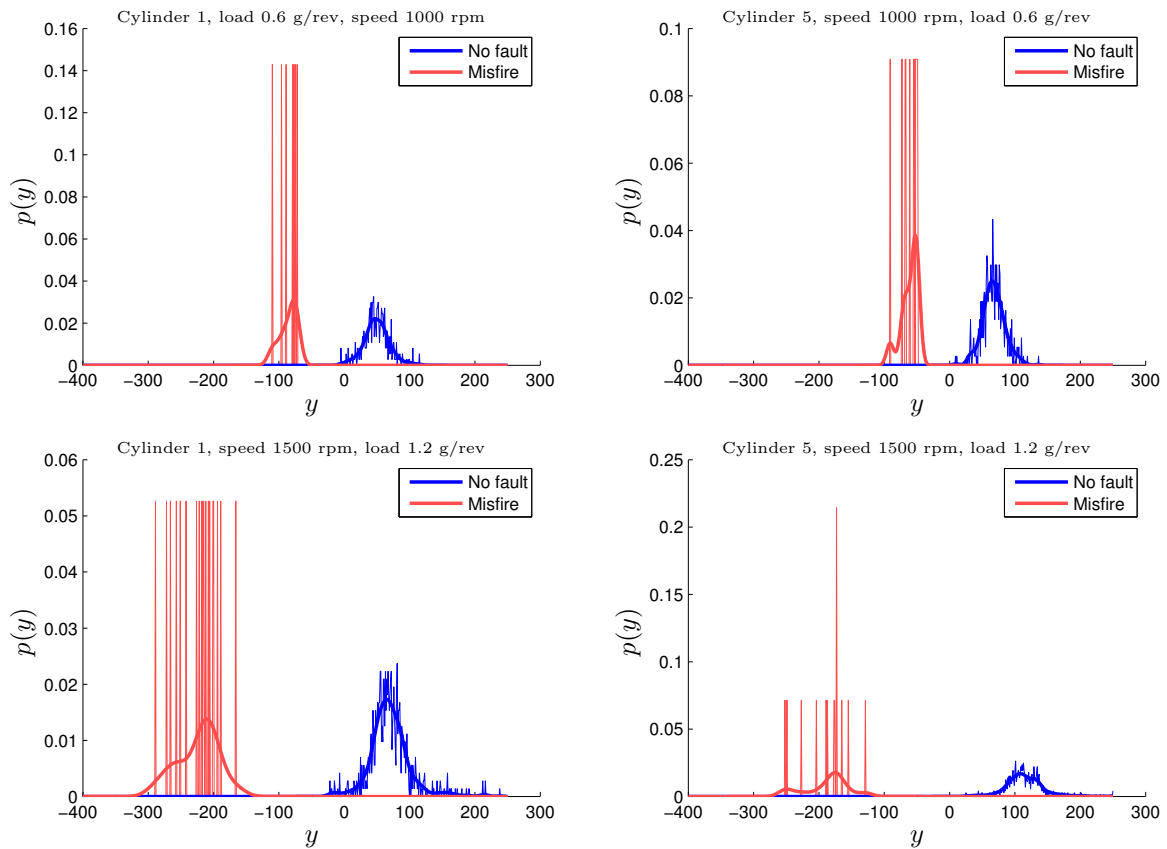


Figure 24: The distribution of the test quantity for different loads, speeds, and cylinders, when maximizing the gap.

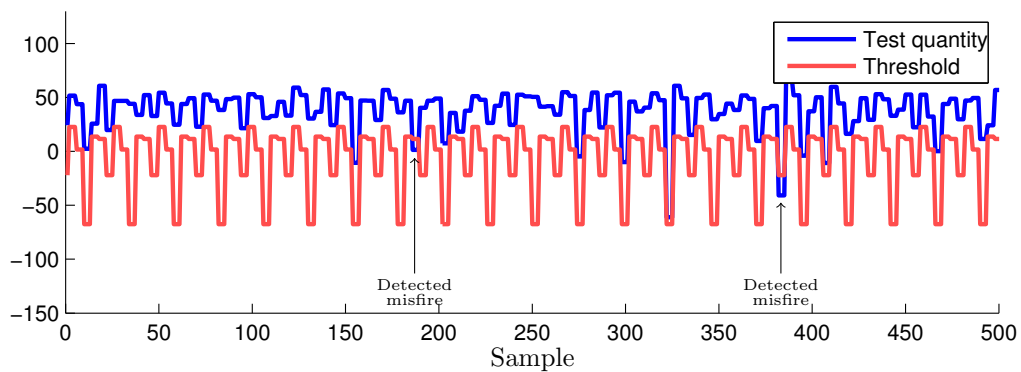


Figure 25: An example of the test quantity and threshold, when maximizing the Kullback-Leibler divergence, for a six cylinder engine during cold start. The threshold variations in the figure depend on the different cylinders.

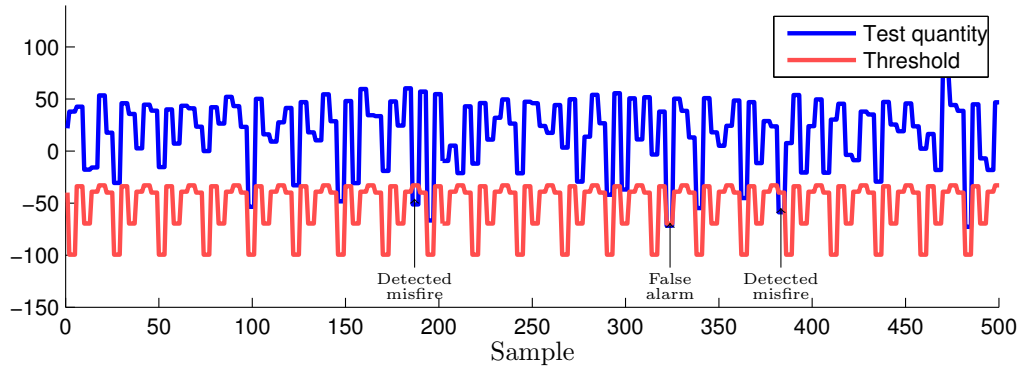


Figure 26: An example of the test quantity and threshold, when maximizing the gap, for a six cylinder engine during cold start. The threshold variations in the figure depend on the different cylinders.

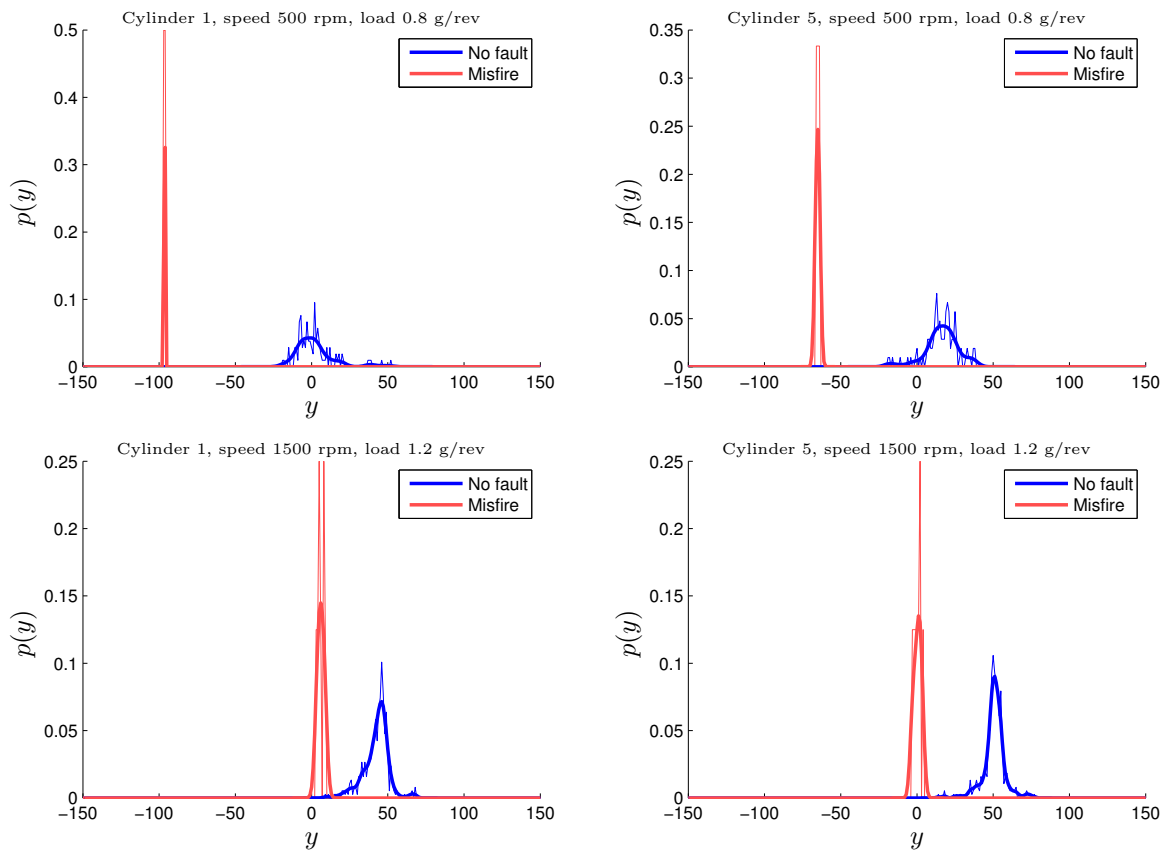


Figure 27: The distribution of the test quantity during cold start for different loads and speeds when maximizing the Kullback-Leibler divergence.

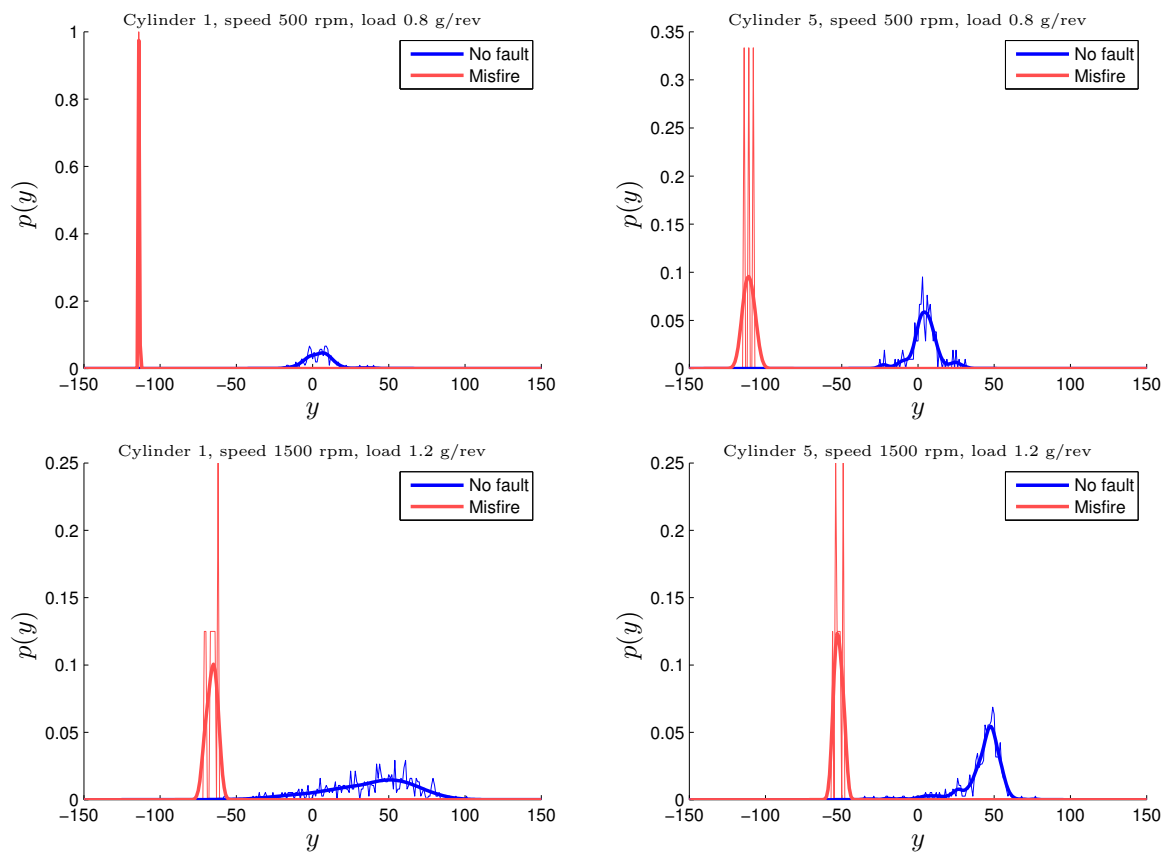


Figure 28: The distribution of the test quantity during cold start for different loads, speeds, and cylinders, when maximizing the gap.

8 Conclusions

A misfire detection algorithm is proposed where the torque at the flywheel is estimated based on the flywheel angular velocity signal. The estimated torque is associated to different operating points depending on speed, load, cylinder, and the catalytic converter warming flag in the vehicle control system. A test quantity is designed by weighting data from each combustion such that the distributions of the test quantity for fault-free data and misfire data are separated. Then, thresholds for detecting misfires are selected for each operating point which balances the probabilities of false alarms and missed detections. All tuning steps are performed automatically given a set of training data which simplifies the tuning of the algorithm.

As a tool for designing and evaluating the misfire detection algorithm, the Kullback-Leibler divergence is proposed. The Kullback-Leibler divergence quantifies the separation between two distributions, in this case describing fault-free data and misfire data, and gives information of when it is easy to detect a misfire. Using the Kullback-Leibler divergence has the advantage that the separation between the distributions is summarized into a scalar value which makes it possible to easily get an overview of the performance of several operating points at the same time. The Kullback-Leibler divergence has proven useful during the whole design process, from analyzing the misfire detectability performance for different samples and operating points to optimizing algorithm parameters.

Two versions of the proposed misfire detection algorithm are evaluated using real data from both a five cylinder engine and a six cylinder vehicle. The difference is how the weights are chosen. In the first version, the weights are chosen such that the Kullback-Leibler divergence is maximized from the misfire data to the fault-free data. In the second version, the weights are chosen such that the gap is maximized between the distributions of the test quantity for the fault-free data and misfire data. The performance of the algorithms are compared to a reference algorithm and evaluations show that the proposed algorithm is able to detect all misfires while having a low probability of false alarms.

9 Future works

In this work, flywheel manufacturing errors that affect the flywheel angular velocity signal are not considered. The errors are different for different vehicles which will affect the results of the misfire detection algorithm. A compensation for these errors should be included in the misfire detection algorithm before it can be used in a production vehicle.

Even though all parameter tuning is performed automatically there are many parameters in the misfire detection algorithm. Both weights for the estimated torque and thresholds at different operating points but also for different cylinders. The number of parameters can possibly be reduced by compensating for the flywheel manufacturing errors. It should be analyzed if the number of parameters can be reduced without significantly degrading the performance of the misfire detection algorithm.

Acknowledgments

The authors would like to thank Sasa Trajkovic at Volvo Cars for helping us with the data collection.

References

- [1] Christopher M. Bishop. *Pattern Recognition and Machine Learning (Information Science and Statistics)*. Springer-Verlag New York, Inc., Secaucus, NJ, USA, 2006.
- [2] Richard H. Byrd, Jean Charles Gilbert, and Jorge Nocedal. A trust region method based on interior point techniques for nonlinear programming. *Mathematical Programming*, 89:149–185, 2000.
- [3] George Casella and Roger L. Berger. *Statistical Inference*. Duxbury Resource Center, Pacific Grove, CA, 2001.
- [4] Francis T. Connolly and Giorgio Rizzoni. Real time estimation of engine torque for the detection of engine misfires. *Journal of Dynamic Systems, Measurement, and Control*, 116(4):675–686, 1994.
- [5] Shinto Eguchi and John Copas. Interpreting Kullback-Leibler divergence with the Neyman-Pearson lemma. *J. Multivar. Anal.*, 97:2034–2040, October 2006.
- [6] Daniel Eriksson, Erik Frisk, and Mattias Krysander. A method for quantitative fault diagnosability analysis of stochastic linear descriptor models. *Automatica*, Accepted for publication.
- [7] Daniel Eriksson, Mattias Krysander, and Erik Frisk. Using quantitative diagnosability analysis for optimal sensor placement. Proceedings of IFAC Safe Process 2012, Mexico city, Mexico, 2012.
- [8] J.B. Heywood. *Internal combustion engine fundamentals*. McGraw-Hill series in mechanical engineering. McGraw-Hill, 1988.
- [9] Ken-jen Lang, Lela Liu, Alec L. Lang, and Louis Yizhang Liu. Multi-Purpose Flywheel (MPF) and Misfire Detection. *SAE Technical Paper 2005-01-1141*, 2005.
- [10] U. Kiencke. Engine misfire detection. *Control Engineering Practice*, 7(2):203 – 208, 1999.
- [11] Kullback, S. and Leibler, R. A. On Information and Sufficiency. *Ann. Math. Statist.*, 22(1):79–86, 1951.
- [12] D. Lundström and S. Schagerberg. Misfire Detection for Prechamber SI Engines Using Ion-Sensing and Rotational Speed Measurements. *SAE Technical Paper 2001-01-0993*, 2001.
- [13] J Mohammadpour, M Franchek, and K Grigoriadis. A survey on diagnostic methods for automotive engines. *International Journal of Engine Research*, 13(1):41–64, 2012.
- [14] Sanjeev Naik. Advanced misfire detection using adaptive signal processing. *International Journal of Adaptive Control and Signal Processing*, 18(2):181–198, 2004.
- [15] Andrew W. Osburn, Theodore M. Kostek, and Matthew A. Franchek. Residual generation and statistical pattern recognition for engine misfire diagnostics. *Mechanical Systems and Signal Processing*, 20(8):2232 – 2258, 2006.
- [16] Francisco V. Tinaut, Andrés Melgar, Hannes Laget, and José I. Domínguez. Misfire and compression fault detection through the energy model. *Mechanical Systems and Signal Processing*, 21(3):1521 – 1535, 2007.

- [17] Andreas Walter, Uwe Kiencke, Stephen Jones, and Thomas Winkler. Misfire Detection for Vehicles with Dual Mass Flywheel (DMF) Based on Reconstructed Engine Torque. *SAE Technical Paper 2007-01-3544*, 2007.